DOKUZ EYLÜL UNIVERSITY
GRADUATE SCHOOL OF NATURAL AND APPLIED SCIENCES

EFFECTS OF SUSPENDED SPRING-MASS SYSTEM ON THE IN-PLANE FREQUENCIES OF FRAME STRUCTURES

by

Hıdır ERKAN

December, 2020
İZMİR

EFFECTS OF
SUSPENDED SPRING-MASS SYSTEM
ON THE IN-PLANE FREQUENCIES OF
FRAME STRUCTURES

A Thesis Submitted to the
Graduate School of Natural and Applied Sciences of Dokuz Eylül University
In Partial Fulfillment of the Requirements for the Degree of Master of Science
in Mechanical Engineering, Machine Theory and Dynamics Program

by
Hıdır ERKAN

December, 2020
İZMİR

M.Sc. THESIS EXAMINATION RESULT FORM

We have read the thesis entitled **“EFFECTS OF SUSPENDED SPRING-MASS SYSTEM ON THE IN-PLANE FREQUENCIES OF FRAME STRUCTURES”** completed by **HIDIR ERKAN** under supervision of **PROF. DR. HASAN ÖZTÜRK** and we certify that in our opinion it is fully adequate, in scope and in quality, as a thesis for the degree of Master of Science.

....

Prof. Dr. Hasan ÖZTÜRK

Supervisor

....

Prof. Dr. Zeki KIRAL

(Jury Member)

....

Dr. Ögr. Üyesi Aysun BALTACI

(Jury Member)

Prof. Dr. Özgür ÖZÇELİK

Director

Graduate School of Natural and Applied Sciences

ACKNOWLEDGMENTS

I would like to remind my venerable esteemed mentor Prof. Dr. Mustafa SABUNCU who I started this study with. He was a wonderful teacher and advisor. I will always remember him.

I would like to express my gratitude to my supervisor Prof. Dr. Hasan ÖZTÜRK who always support and help me with understanding and patience.

I would like to thank Research Assistant Salih DEMİRTAŞ and Research Assistant Seda VATAN for their valuable help.

I owe my deepest gratitude to my family who has given me support throughout my life.

Hıdır ERKAN

EFFECTS OF SUSPENDED SPRING-MASS SYSTEM ON THE IN-PLANE FREQUENCIES OF FRAME STRUCTURES

ABSTRACT

In this study, effects of the suspended mass-spring system on the in-plane natural frequencies, mode shapes and dynamic stability of multi-bay frame structures were investigated. The frame structures were modeled by the finite element method based on the Euler-Bernoulli beam theory. Suspended mass-spring systems are assumed to move only in the vertical direction.

The finite element model of the system was created and code was created in the MATLAB program for its solution. The results are compared with the results obtained from ANSYS program. The results obtained in the analyses are given in graphs and tables. Effects of the number, position and spring stiffness of the mass-spring system on the frequency values, mode shapes and dynamic stability of frame structures were determined. In addition, when the natural frequency of the suspended mass-spring system is greater or smaller than the first natural frequency of the frame structures, it is reacted that it affects the natural frequency of the frame structures differently.

Keywords: Free vibration, dynamic stability, finite element method, suspended spring-mass, multi-bay frames

ASILI KÜTLE-YAY SİSTEMİNİN ÇERÇEVE YAPILARIN

DÜZLEM İÇİ DOĞAL FREKANSLARI ÜZERİNDEKİ ETKİLERİ

ÖZ

Bu çalışmada, asılı kütle-yay sisteminin çok bölmeli çerçeve yapıların düzlem içi doğal frekanslarına, titreşim biçimlerine ve dinamik kararlılığına olan etkileri incelenmiştir. Çerçeveler, Euler-Bernoulli kiriş teorisi kullanılarak sonlu elemanlar yöntemiyle modellenmiştir. Asılı kütle-yay sistemlerinin sadece düşey doğrultuda hareket ettiği kabul edilmiştir.

Sistemin sonlu elemanlar modeli oluşturulmuş ve çözümü için MATLAB programında kod yazılmıştır. Sonuçlar ANSYS programından elde edilen sonuçlarla karşılaştırılmıştır. Yapılan analizlerde elde edilen sonuçlar grafikler ve tablolar halinde verilmiştir. Kütle-yay sistemi sayısının, konumunun ve yay direngenliğinin çerçeve yapıların frekans değerleri, titreşim biçimleri ve dinamik kararlılığı üzerindeki etkileri tespit edilmiştir. Ayrıca asılı kütle-yay sisteminin doğal frekansının, çerçeve yapıların ilk doğal frekansından büyük ya da küçük olduğu durumlarda, çerçeve yapıların doğal frekansını farklı etkilediği tespit edilmiştir.

Anahtar Kelimeler: Serbest titreşim, dinamik kararlılık, sonlu elemanlar yöntemi, asılı kütle-yay, çok bölmeli çerçeveler

CONTENTS

Page

LIST OF FIGURES

Page

LIST OF TABLES

Page

CHAPTER ONE

INTRODUCTION

1.1 Introduction

Frame structures constitute the framework of the structures in many advanced engineering fields such as bridges, buildings, load-bearing systems, land, sea and air vehicles. The behavior of engineering structures against static and dynamic loads that they are exposed to during their operating period depends on the behavior of the framework structures. Vibration in buildings with external dynamic forcing may cause great damage to buildings in the long term. Therefore, it is important to determine the critical loads, free vibration responses and stable regions where the elements can work safely by examining the behavior of the structural elements under static and dynamic loads.

In this study, free vibration responses and dynamic stability conditions of single and multi-bay frame structures are investigated for cases with and without a suspended mass-spring system. In addition, effects of the number, position and resistance coefficient of suspended mass-spring systems on the system were also examined. Such structures appear in the aircraft wings, which are exemplified in Figure 1.1 in practice. The airplane wing framework is a good example of frame structures. The engine and its connections suspended on the aircraft wing can also be considered as the suspended mass-spring. In this case, the behavior of the wing during operation can be given as an example of the main subject of this study.

Figure 1.1 An example of structures with suspended mass-spring system (Airbus, 2020)

1.2 Literature Review

The free vibration responses and mode shapes of the frame structures have been examined by many researchers, also examined rod behavior by adding suspended mass-spring on the rods. Likewise, some researchers have examined the dynamic stability regions of frame structures. A few of these researches in this direction are given below:

Kapur (1966) calculated the vibration analysis of the Timoshenko bar using the finite element method by using a beam element containing shear force and rotational inertia effects.

Thomas & Belek (1977) explored the free vibration behavior of frame structure by using the finite element method. In their study, they examined effects of weight, flexural rigidity and ratios between the columns and beams on the free vibration of frame structures.

Kawashima & Fijimato (1984) improved a mathematical model assumed that semi-solid connections between the elements of the frame systems. This model represents that each element contains a flexible beam with absorber and spring ends. For this model, the dynamic stiffness matrix of the beam element is obtained. The direct stiffness method was applied to the frame system with semi-rigid joints. Experimental studies were carried out on frame to confirm the method of analysis.

Lee & HG (1994) studied by using the Rayleigh-Ritz principle, the natural frequencies and mode shapes of various frame structures have been calculated. For the portal frame, the results of the numerical solution are very close with the exact numerical solution.

Mei (2012) studied the free vibration of multi-bay frame structures. They used a wave vibration approach to solve the problem. The vibration is described as waves propagating along with beam elements.

Erkan, Öztürk & Sabuncu (2013) examined in-out plane mode shapes and free vibration frequencies of the multi-bay frames. They found and rule out effects of the number of bays, column angles, and the cross-section change of columns on the free vibration response.

Gürgöze (1996) investigated the frequency equation of the Bernoulli-Euler beam carried a lumpy mass and a suspended mass-spring at the end by using the Lagrange multipliers method.

Qiao, Li & Li (2002) investigated a new method for free vibration analysis of non-uniform Euler–Bernoulli beams with suspended spring–mass systems.

Erkan, Öztürk & Demirtaş (2019) investigated effects of the suspended spring-mass system on the in-plane frequencies and mode shapes of frame structures. In the study, frame structures were modeled according to Bernoulli-Euler's theory. They observed changes in the frequency and mode shapes of the frame structures by adding mass-spring systems in different numbers and positions to the frame systems and changing the stiffness coefficient of the mass-spring systems.

Sarsmaz (2016) investigated the effects of the suspended spring-mass system on in-plane natural frequencies in a curved beam with different torsional foundation conditions using the finite element method. In the study, the curved beam is modeled using the Euler beam, and the spring-mass systems are only allowed to displace in the vertical direction.

Bolotin (1962) systematically presented the general theory of the dynamic stability of elastic systems, demonstrated how to analyze the dynamic instability regions of a beam subjected to periodic axial load, and set up the necessary equations for boundary frequencies.

Thomas & Abbas (1975), (1976) developed a finite element model for the stability analysis of the Timoshenko beam subjected to periodic axial loads and shear deformation on the static buckling loads.

Abbas (1977) used the finite element method to investigate the stability problem of complex structures subjected to external loads.

Briseghella, Majorana & Pellegrino (1998) studied to find regions of dynamic stability of frames by using the finite element method. The numerical approach given in the study, allowed to obtain the diagrams in which these regions are located taking into account the constraints, inertia and stiffness characteristics of the dynamic force applied and the vibration frequency of the analyzed structures.

Öztürk, Yashar & Sabuncu (2016) investigated the effects of crack depth, crack location and number of bays on the dynamic and static stability of in-plane multi-bay frame structures under periodic load.

Vatan (2019) investigated the effects of the number, location and stiffness coefficient of suspended spring-mass systems on dynamic stability of curved beams for both isotropic material and layered composite at different subtended angles and different radius.

As a result of the investigations given above, considering that the deficiencies in the literature will be eliminated, effects of suspended spring-mass systems in frame systems on in-plane natural frequencies, mode shapes and dynamic stability of frame structures have been investigated and the results have been examined.

1.3 Objective of the Thesis

In this study, effects of suspended mass-spring systems on the responses of free vibration and dynamic stability regions of multi-bay frames were investigated**.**

First, the frame structures with the suspended spring-mass system were modeled using the finite element method and then the system matrices were determined according to the energy equations. Then, buckling and frequency analysis were performed. Finally, effects of the stiffness coefficients, the position and number of the spring-mass system on the free vibration responses and dynamic stability regions of the frame structures were investigated. The results were explained with tables and graphs.

1.4 Outline of the Thesis

This study consists of seven chapters. In the study, literature studies on similar topics are given in Chapter 1. Chapter 2 discusses the finite element method. The dynamic stability theory is explained in Chapter 3. In Chapter 4, the theoretical solution to the problem is given. In Chapter 5, the free vibration frequencies and mode shapes of the frames are given in graphs and tables. In Chapter 6, dynamic stability analysis answers are given and the results are examined. Finally, Chapter 7 includes the conclusion of the study.

CHAPTER TWO

THEORY OF THE FINITE ELEMENT METHOD

2.1 The Finite Element Method

The finite element method is a kind of solution in which complex problems are divided into simpler sub-problems and each solution is solved in itself. Due to this feature, the finite element method has been widely used in many engineering fields in the last century. The method was used in 1950 for stress analysis in the aircraft and space industries. As a result of the studies on the principles of the method, the field of use has been expanded and it is widely used in different fields from biomechanics to nuclear technology with advancing computer technology. Nowadays, the finite element method is mostly preferred in researches for structural analysis as seen in Figure 2.1.

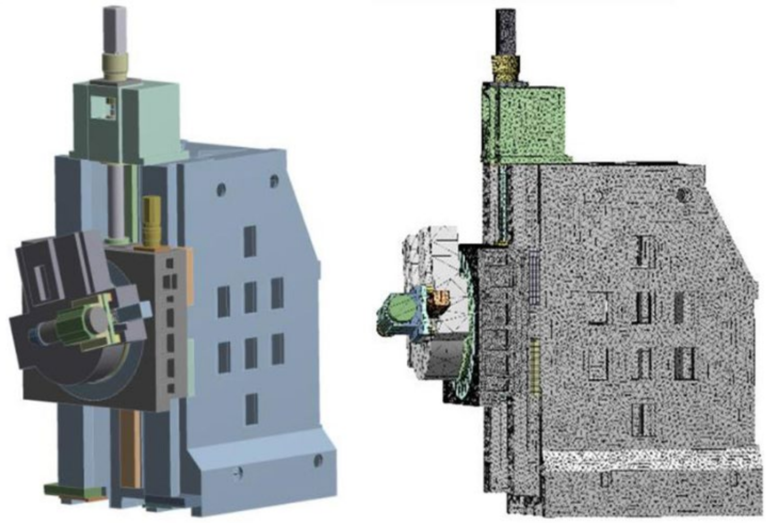

Figure 2.1 Finite element model of a machine (Ji, Sun, & Huang, 2018)

In the finite element method, an examined structure is divided into elements defined previously finite element. The process of dividing the structure into small pieces is named 'meshing'. The finite elements are the fundamental elements that cannot be divided into smaller elements. The structure is redefined by joining the finite elements at the nodes. This coupling process is defined mathematically by algebraic equations. Algebraic equations are solved and results are obtained. All of this process is defined as a finite element analysis.

2.2 The Finite Element Analysis Processes

A finite element analysis consists of three main topics called preprocess, process and post-process. These basic topics are the algorithm for creating, solving and interpreting the results. Each title consists of several steps.

2.2.1 Preprocess

Preprocess is the section where the problem is defined, the appropriate finite element is selected. The meshing process is performed and the boundary conditions are created. This section consists of six stages.

a) Select Analysis Type

At this stage, the problem is identified and the type of analysis is selected. Some analyses to be done using the finite element method can be listed as follows; modal analysis, buckling analysis, transient dynamic analysis, structural static analysis, steady-state thermal analysis, transient thermal analysis. After selecting the analysis type, the model is created.

b) Select Element Type

According to the structure to be analyzed, the finite element to be used is selected. While making this selection, it is decided whether to a two-dimensional or three-dimensional analysis. This choice is related to the type of problem and the structure to be analyzed. Elements selected in two and three-dimensional analyses can be linear or quadratic. Quadratic finite elements are defined by two-degree equations. The purpose of using this element is to increase the accuracy of the results to be obtained. The basic elements used in the finite element method are bar, beam, shell, plane and solid elements.

The bar element shown in Figure 2.2 is an element consisting of two nodes and two degrees of freedom. This element carries loads only in axial the direction and undergoes deformation.

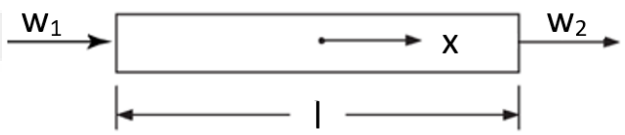

Figure 2.2 A bar element

The beam element shown in Figure 2.3 is an element consisting of two nodes and four degrees of freedom. The beam element is deformed only in the direction perpendicular to its axis. The difference between the beam and the cage element is the type of load they carry. The beam element is subjected to transverse forces and moments, that is, they are loaded transversely, so they are deformed transversely.

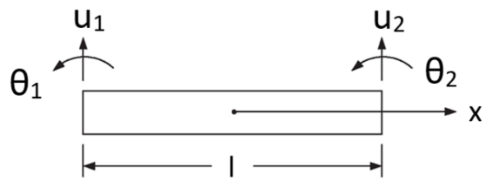

Figure 2.3 A beam element

Shell element shown in Figure 2.4 can be square or triangular. Their thickness is quite small compared to other dimensions. They cannot be loaded vertically.

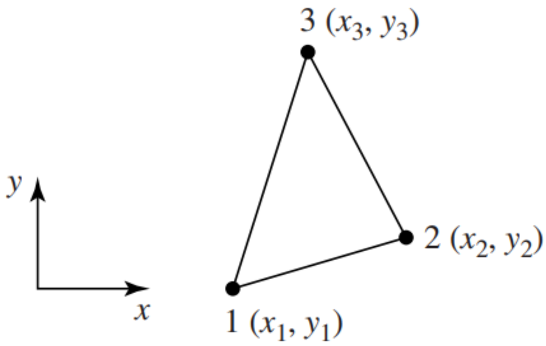

Figure 2.4 A shell elements (Hutton, 2004)

Plane elements show the properties of the shell element. The difference from the shell element is that the rotation around the knot point is neglected. Not suitable for loads perpendicular to the plane.

Solid element shown in Figure 2.5 is three-dimensional elements. The inside angle of each corner of the element surface must be less than 180°. The best results are obtained when it is between 45° and 135°. The length ratio of the long edge to the short edge should not be much. The best results are obtained when the sides are equal or the aspect ratio is less than four, and the aspect ratio should not exceed ten should not exceed.

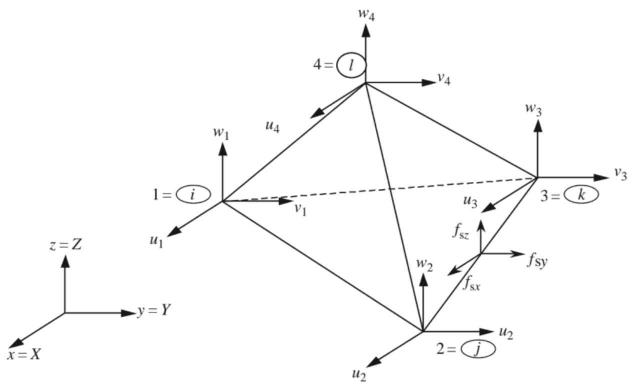

Figure 2.5 A solid element (Liu, & Quek, 2003)

c) Define Material Properties

At this stage, properties such as elasticity module, Poisson’s ratio, density, shear modulus, which are the main properties of the material, are defined.

d) Meshing

Mesh is a network of cells and dots. Mesh elements can be very different in size and shape and are used in the solution of partial differential equations. When mesh elements are combined, the equation that needs to be solved for the entire system is provided.

Due to the complexity of the system under consideration, it may be impossible to solve the entire system without breaking it into small pieces. The details such as corner, hole and slope in the system examined can make it difficult to obtain solutions. For this reason, small and defined elements are relatively easy to solve and are therefore a preferred method.

In complex geometries as exemplified in Figure 2.6, meshing is done with computer-aided ready-made programs. But in simple geometry, meshing is done manually and the created equations are solved with the help of computers. The solution to the problems described in this study was done in both ways. MATLAB and Ansys programs were used for this issue.

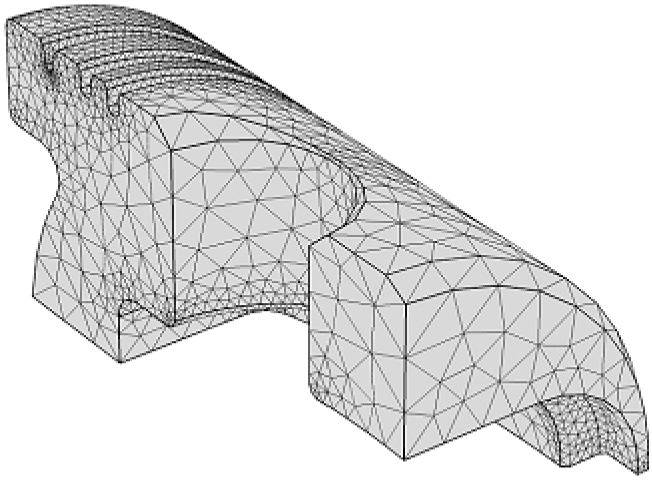

Figure 2.6 A mesh model (Griesmer, 2014)

e) Building elements by Assigning Connectivity

The model divided into finite elements is re-modeled by joining the elements. This process mathematically corresponds to combining the differential equation in each element. The element matrices defined for each element are placed in the appropriate rows and columns in the general metric that defines the entire system, and the general matrix of the system is created. The size of this matrix is equal to the degree of freedom of the system.

f) Applying Boundary Conditions and Loads

A boundary condition limits the degree of freedom at the fixing point of the system under examination. Boundary conditions are applied by deleting rows and columns appropriate to the system general matrix.

The forces acting on the system are written as a vector matrix and replaced in the equation.

2.2.2 Processing

When the above steps are completed, the mathematical model is created according to the finite element method of the examined structure. The next step is solving the equation. In general, the solution is made with the help of a computer since the size of the system matrix is large.

2.2.3 Post-processing

The results obtained at this stage are interpreted and judgments are made about the structure examined.

CHAPTER THREE

THEORY OF DYNAMIC STABILITY

The definition of stability means resisting change in a broad sense. The stability of the systems can be static or dynamic. Static stability is related to the return of the disturbed system to its original position. Dynamic stability is related to how long it takes the system to return to its original position. Static stability problems are examined when structures are exposed to a static load. If static loads are higher than a certain value, the structure will be buckled. This load is called the critical buckling load. If the applied loads are time-dependent, the situation turns into a dynamic stability problem. As a result, the forces applied to the systems generally consist of two components, one is static load and the other is dynamic load. For this reason, static and dynamic stabilities of the structures are examined.

3.1 Theory of Stability

Figure 3.1 is taken into account to explain the theory of stability. The lumped mass is fixed at the end of the unweighted bar. The movement of the bar is limited to the b sign. If the position of the mass at any moment is defined by y, the strength of the rod to restore its resilience becomes -ky, and the motion equation is written as follows.

$$-ky = m\ddot{y} \tag{3.1}$$

k in Equation 3.1 is the stiffness coefficient of the system and its equivalent is given in Equation 3.2 (Abbas, 1977).

$$k = \frac{3EI}{l^3} \tag{3.2}$$

I is the moment of inertia and E is the modulus of elasticity. Substituting Equation 3.2 into Equation 3.1

$$\ddot{y} + \frac{3EI}{ml^3} y = 0 \tag{3.3}$$

Equation 3.3 is the free vibration equation of the mass m.

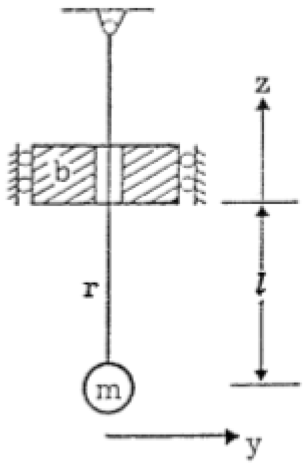

Figure 3.1 Mechanical System (Abbas, 1977, p.69)

If the position of the bushing is assumed to change, the movement equation of the bushing is written as follows depending on the time:

$$z = Acos\omega t \tag{3.4}$$

In this case, the stiffness of the system becomes time dependent.

$$k = \frac{3EI}{(l+z)^3} = \frac{3EI}{(l + Acos\omega t)^3} \tag{3.5}$$

Equation 3.3 is then was rebuilt

$$\ddot{y} + \frac{3EI}{m(l + Acos\omega t)^3} y = 0 \tag{3.6}$$

Since there is no external force acting on the system, vibration is not forced vibration. However, since the change of stiffness creates a force on the system. In this case, the type of vibration is not the free vibration. This form of vibration due to the parameters of the system is called parametric vibration. The parametric vibration declaration is as follows.

$$\frac{d^2y}{d\tau^2} + (a - 2bcos2\tau)y = 0 \tag{3.7}$$

where a and b values in the equation are constant.

From Equation 3.6 and Equation 3.7, the stiffness of the system can be written as

$$k = \frac{3EI}{(l + Acos\omega t)^3} = \frac{3EI}{l^3}\left(1 - \frac{3A}{l} cos\omega t\right) \tag{3.8}$$

In this case, Equation 3.6 is

$$\ddot{y} + \frac{3EI}{ml^3}\left(1 - \frac{3A}{l} cos\omega t\right) y = 0 \tag{3.9}$$

If the Equation 3.9 is rewritten in dimensionless time,

$$\frac{d^2y}{d\tau^2} + \left(\frac{12EI}{m\omega^2 l^3} - \frac{36EIA}{m\omega^2 l^4} cos2\tau\right) y = 0 \tag{3.10}$$

Here, a and b can be written as follows,

$$a = \frac{12EI}{m\omega^2 l^3} \quad and \quad b = \frac{18EIA}{m\omega^2 l^4} \tag{3.11}$$

Equation 3.7 is known as the Mathieu equation. Figure 3.2 can be recognized in two characteristic solutions to this equation. As seen in Figure 3.2, the results depend on parameters a and b. While vibration amplitudes are limited in some values of a and b parameters, vibration amplitudes increase in other values. The difference between the first and the second case is the value taken by the parameter a. In the first case, vibration amplitudes increase, in the second case, the amplitudes remain constant. As can be seen from the results, the important thing is the trend followed by the vibration process. If the amplitudes are limited, the system is stable. Otherwise, parametric resonance occurs and the system becomes dynamically is stable.

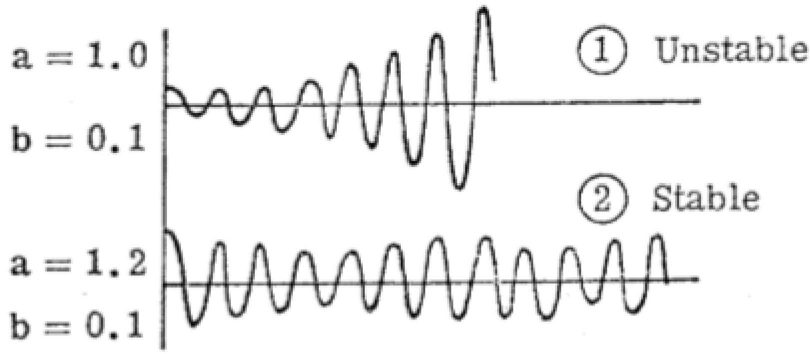

Figure 3.2 Two Solutions of Mathieu’s Equation (Abbas, 1977, p.69)

Three causes of parametric excitation can be seen as follows:

a) periodic change in rigidity

b) periodic change in inertia of the system and

c) periodic change in the loading of the system

In this study, periodically changing external force is applied to the examined systems. Therefore, only one of effect that cause parametric vibration has been taken into account.

3.2 A System with Periodic Load

Given the system shown in Figure 3.3, the mass (m) is connected to the upper end of a perfectly resistant vertical rod (r) and the lower end of the rod is connected to hinged support that provides elastic resistance to rotation. The vertical force P acts on the upper end of the bar**.**

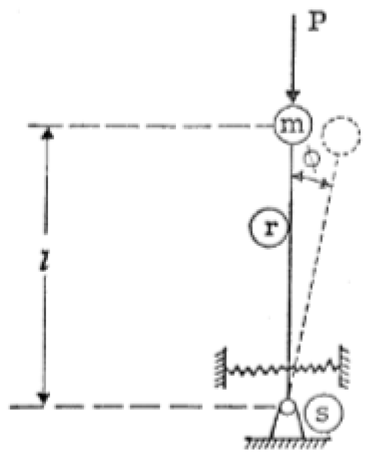

Figure 3.3 The system with periodic change in loading (Abbas,1977,p.70)

The free vibration equation of the system in Figure 3.3 is as follows.

$$Pl\Phi - k\Phi = ml^2\ddot{\Phi} \tag{3.12}$$

where k is the restoring moment and the weight of the mass is included in the P force.

If the force P changes harmonically,

$$P(t) = P_0 + P_t cos\omega t \tag{3.13}$$

In this case, Equation 3.12 can be rewritten as follows,

$$\ddot{\Phi} + \frac{1}{ml^2}(k - P_0 l - P_t cos\omega t)\Phi = 0 \tag{3.14}$$

where

$$2\tau = \omega t\,, \qquad a = \frac{4}{m\omega^2 l^2}\left(\frac{k}{l} - P_0\right), \quad b = \frac{2P_t}{m\omega^2 l} \tag{3.15}$$

CHAPTER FOUR

THEORETICAL ANALYSIS

In this section, finite element solution steps of frame structures are explained. The frame system is formed from uniform cross-section beams and the Euler-Bernoulli beam approach has been adopted. In the analyses, it is assumed that the frame only vibrates in the plane.

4.1 Problem Description

The frame structure used in this study is shown in Figure 4.1. The element used as a column and beam in frame structures is given in Figure 4.2. Figure 4.1 shows how to connect columns and beam and fix the frame structure. The mass-spring system used in the study is given in Figure 4.3 and how it is connected to the frame structures is shown. The stiffness coefficient (k_s) and mass (m_s) symbols of the suspended mass-spring system are given on the figure.

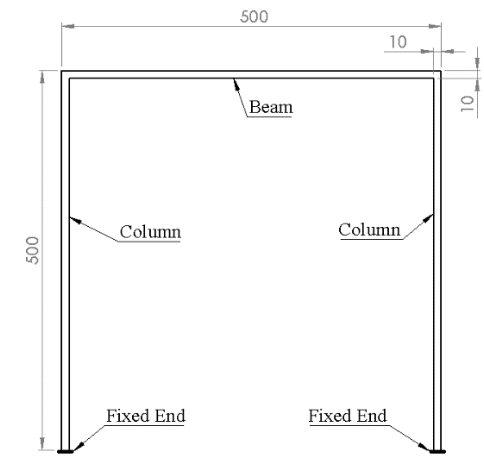

Figure 4.1 The frame structure

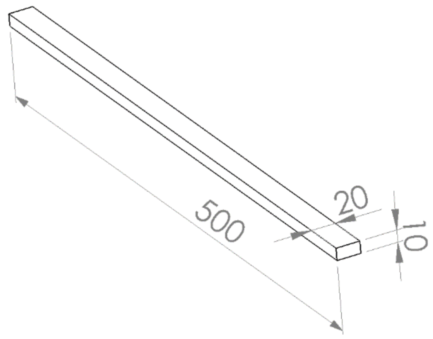

Figure 4.2 The column and beam elements

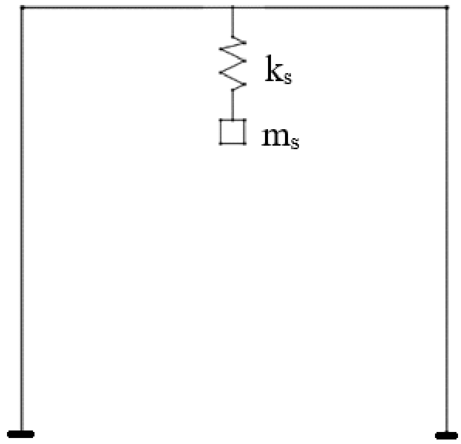

Figure 4.3 Frame structure with the suspended spring-mass system

4.2 The Finite Element Model

The frame system is modeled with the frame finite element. The frame element consists of a combination of bar and beam elements. First of all, the motion equations of the bar and beam elements were formed and the mass and stiffness matrices of these elements were found. Then, the mass and stiffness matrix of the frame element is derived regarding the bar and beam elements. Then, how the global matrix of the frame structure is created is explained. Finally, the mass and stiffness matrix of the suspended spring-mass system is given and how it is added to the global matrix is explained.

4.2.1 Bar Element

The bar element shown in Figure 4.4 moves only in the x-axis direction and has two freedom degrees. The element length is $\boldsymbol{\ell}$.

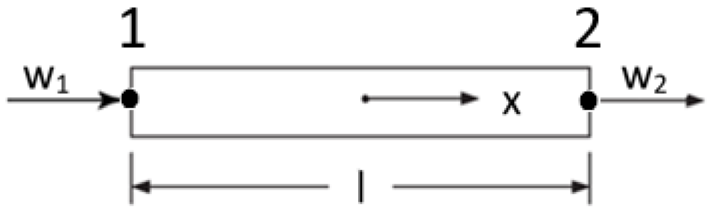

Figure 4.4 A bar element with nodes

The shape function of the bar element show in Equation 4.1

$$w(x,t) = a_1(t) + a_2(t)x \tag{4.1}$$

Joint displacements of bar element are shown in Figure 4.2,

$$w(0,t) = w_1(t)\,,\;\; w(l,t) = w_2(t) \tag{4.2}$$

the constants a_1 and a_2 are given in as in Equation 4.3 and 4.4.

$$w_1(t) = a_1(t) \;\; or \;\; a_1(t) = w_1(t) \tag{4.3}$$

$$w_2(t) = a_1(t) + a_2(t)l \;\; or \;\; a_2(t) = \frac{w_2(t) - w_1(t)}{l} \tag{4.4}$$

If the constants are substituted in Equation 4.1, the shape function are obtained;

$$w(x,t) = w_1(t)\left(\frac{1-x}{l}\right) + w_2(t)\frac{x}{l} \tag{4.5}$$

The kinetic energy equation for the longitudinal vibration as follows

$$T = \frac{1}{2}\rho A\left(\frac{\partial w}{\partial t}\right)^2 dx \tag{4.6}$$

ρ is density of the material

A is the cross-section area of the bar element.

When Equation 4.6 is rearranged, take the following figure;

$$T = \frac{1}{2}\frac{\rho Al}{3}({\dot{w}_1}^2 + \dot{w}_1\dot{w}_2 + {\dot{w}_2}^2) \tag{4.7}$$

Where,

$$\dot{w}_1 = \frac{dw_1(t)}{dt} \quad and \quad \dot{w}_2 = \frac{dw_2(t)}{dt} \tag{4.8}$$

If the joint displacements are represented as a vector,

$$\dot{w} = \begin{Bmatrix} \dot{w}_1 \\ \dot{w}_2 \end{Bmatrix} \tag{4.9}$$

in this case, Equation 4.6 is rewritten as follows,

$$T = \frac{1}{2}\dot{w}^T m \dot{w} \tag{4.10}$$

m is the mass matrix of bar element,

$$m = \frac{\rho A l}{6}\begin{bmatrix} 2 & 1 \\ 1 & 2 \end{bmatrix} \quad (4.11)$$

The strain energy is

$$V = \frac{1}{2} EA \left(\frac{\partial w}{\partial x}\right)^2 dx \quad (4.12)$$

E is the elasticitty module of material. The strain energy of the element can be written as,

$$V = \frac{1}{2} EA \int_0^l \left(-\frac{1}{l} w_1(t) + \frac{1}{l} w_2(t)\right)^2 dx \quad (4.13)$$

$$V = \frac{1}{2}\frac{EA}{l}(w_1^2 - 2w_1 w_2 + w_2^2) \quad (4.14)$$

The displacement vector is

$$w = \begin{Bmatrix} w_1 \\ w_2 \end{Bmatrix} \quad (4.15)$$

Equation 4.12 is rewritten as follows

$$V = \frac{1}{2} w^T k w \quad (4.16)$$

Finally, the stiffnes matrix of the bar element is obtained.

$$k = \frac{EA}{l}\begin{bmatrix} 1 & -1 \\ -1 & 1 \end{bmatrix} \tag{4.17}$$

4.2.2 Beam Element

The beam element is shown in Figure 4.5 has two nodes and four degrees of freedom. The beam element is capable of carrying transverse forces and moments. The length of the beam element is indicated by *l*.

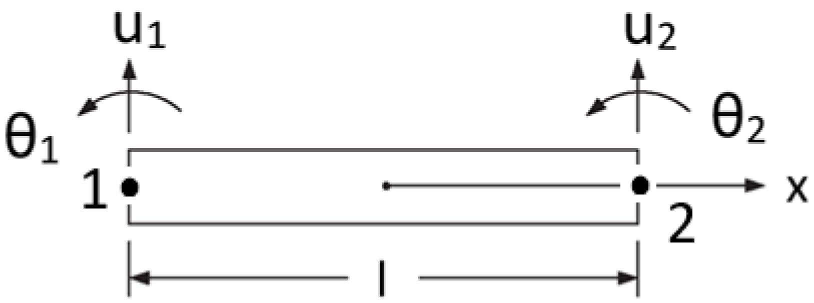

Figure 4.5 A beam element with nodes

The shape function of a beam element can be represented as

$$u(x,t) = a_1(t) + a_2(t)x + a_3(t)x^2 + a_4(t)x^3 \tag{4.18}$$

Boundary conditions are given as follows,

$$u(0,t) = u_1(t)\,, \qquad \acute{u}(0,t) = u_2(t)\,, \qquad u(l,t) = u_3(t)\,, \qquad \acute{u}(l,t) = u_4(t) \tag{4.19}$$

The shape function constants, $a_1(t)$, $a_2(t)$, $a_3(t)$, and $a_4(t)$, are described as

$$a_1(t) = u_1(t) \tag{4.20}$$

$$a_2(t) = u_2(t) \tag{4.21}$$

$$a_3(t) = \frac{1}{l^2}[-3u_1(t) - 2u_2(t)l + 3u_3(t) - u_4(t)l] \tag{4.22}$$

$$a_4(t) = \frac{1}{l^3}[2u_1(t) + u_2(t)l - 2u_3(t) + u_4(t)l] \tag{4.23}$$

By substituting Equation 4.23 into Equation 4.18, *u(x,t)* is,

$$\begin{aligned} u(x,t) = &\left(1 - 3\frac{x^3}{l^2} + 2\frac{x^3}{l^3}\right)u_1(t) + \left(\frac{x}{y} - 2\frac{x^2}{l^2} + \frac{x^3}{l^3}\right)lu_2(t) \\ &+ \left(3\frac{x^2}{l^2} - 2\frac{x^3}{l^3}\right)u_3(t) + \left(-\frac{x^2}{l^2} + \frac{x^3}{l^3}\right)lu_4(t) \end{aligned} \tag{4.24}$$

If the displacement terms are renamed as,

$$N_1 = 1 - 3\frac{x^2}{l^2} + 2\frac{x^3}{l^3} \tag{4.25}$$

$$N_2 = (\frac{x}{l} - 2\frac{x^2}{l^2} + \frac{x^3}{l^3})l \tag{4.26}$$

$$N_3 = 3\frac{x^2}{l^2} - 2\frac{x^3}{l^3} \tag{4.27}$$

$$N_4 = (-\frac{x^2}{l^2} + \frac{x^3}{l^3})l \tag{4.28}$$

N_1,N_2,N_3 and N_4 are the shape functions. Equation 4.24 can be edited as follows,

$$u(x,t) = [N_1\ N_2\ N_3\ N_4] \begin{Bmatrix} u_1 \\ u_2 \\ u_3 \\ u_4 \end{Bmatrix} \tag{4.29}$$

$$u(x,t) = Nu \tag{4.30}$$

The kinetic energy equation is

$$T = \frac{1}{2}\int_0^l \rho\, A \left\{\frac{\partial u(x,t)}{\partial t}\right\}^2 dx \tag{4.31}$$

$$T = \frac{1}{2}\dot{u}^T m \dot{u} \tag{4.32}$$

m is the mass matrix of beam element and it can be written as follow,

$$m = \frac{\rho A l}{420}\begin{bmatrix} 156 & 22l & 54 & -13l \\ 22l & 4l^2 & 13l & -3l^2 \\ 54 & 13l & 156 & -22l \\ -13l & -3l^2 & -22l & 4l^2 \end{bmatrix} \tag{4.33}$$

The potential energy is defined as

$$V = \frac{1}{2}EI\left\{\frac{\partial^2 u(x,t)}{\partial x^2}\right\}^2 dx \tag{4.34}$$

If the *u(x,t)* is written into Equation 4.34

$$V = \frac{1}{2} EI \int_0^l \left(-\frac{1}{l} u_1(t) + \frac{1}{l} u_2(t) \right)^2 dx \tag{4.35}$$

$$V = \frac{1}{2} u^T k u \tag{4.36}$$

k is the stiffness matix of beam elemant,

$$k = \frac{EI}{l^3} \begin{bmatrix} 12 & 6l & -12 & 6l \\ 6l & 4l^2 & -6l & 2l^2 \\ -12 & -6l & 12 & -6l \\ 6l & 2l^2 & -6l & 4l^2 \end{bmatrix} \tag{4.37}$$

4.2.3 Frame Element

The frame element shown in Figure 4.6 has two nodes and six degrees of freedom. The frame element takes both transverse forces and axial, as well as moments. The frame element is a combination of the bar and beam elements. The element length is *l*, cross-section area is *A*, modulus of elasticity is *E*, the density is ρ and the inertia moment is *I*.

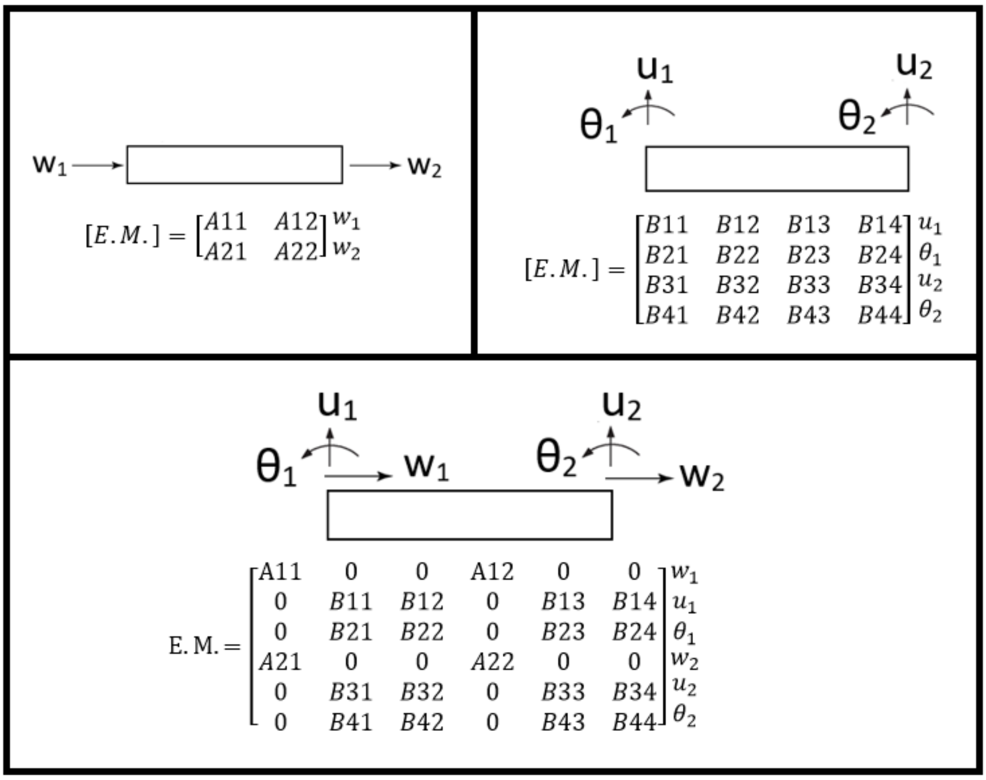

Figure 4.6 Combine bar and beam elements (E.M.: Element Matrix)

The matrices of the frame elements can be obtained from Equations (4.11), (4.17), (4.33) and (4.37).

$$\mathrm{m} = \frac{\rho \mathrm{Al}}{420}\begin{bmatrix} 140 & 0 & 0 & 70 & 0 & 0 \\ 0 & 156 & 22l & 0 & 54 & -13l \\ 0 & 22l & 4l^2 & 0 & 13l & -3l^2 \\ 70 & 0 & 0 & 140 & 0 & 0 \\ 0 & 54 & 13l & 0 & 156 & -22l \\ 0 & -13l & -3l^2 & 0 & -22l & 4l^2 \end{bmatrix} \qquad (4.38)$$

$$
k = \frac{\rho \mathrm{Al}}{420}\begin{bmatrix} \frac{AE}{l} & 0 & 0 & -\frac{AE}{l} & 0 & 0 \\ 0 & \frac{12EI}{l^3} & \frac{6EI}{l^2} & 0 & -\frac{12EI}{l^3} & -\frac{6EI}{l^2} \\ 0 & \frac{6EI}{l^2} & \frac{4EI}{l} & 0 & -\frac{6EI}{l^2} & \frac{2EI}{l} \\ \frac{AE}{l} & 0 & 0 & \frac{AE}{l} & 0 & 0 \\ 0 & \frac{12EI}{l^3} & -\frac{6EI}{l} & 0 & \frac{12EI}{l^3} & -\frac{6EI}{l^2} \\ 0 & \frac{6EI}{l^2} & \frac{2EI}{l} & 0 & -\frac{6EI}{l^2} & \frac{4EI}{l} \end{bmatrix} \tag{4.39}
$$

4.2.4 Transformation Matrix

The matrices formulated above are for the finite element in a specific coordinate. Generally, a frame consists of elements in different orientations. The first coordinate system of the finite elements is called the local coordinate system. To create the frame system by bringing together the finite elements, it is first necessary to transform the local element coordinates to the global coordinate system, as in Figure 4.7. In this way, all elements are expressed in a common coordinate system.

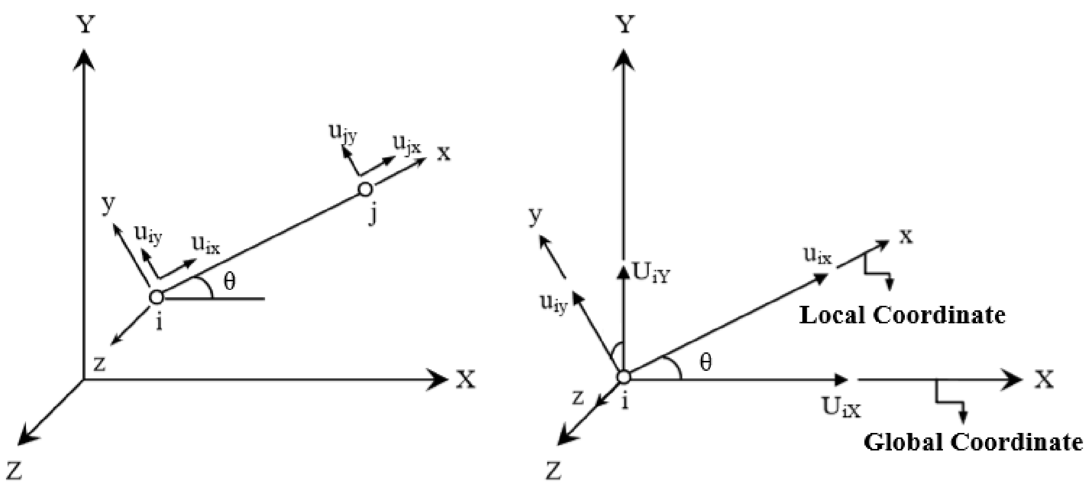

Figure 4.7 Transformations from local to global coordinate

$$
L = \begin{bmatrix} \cos\theta & \sin\theta & 0 & 0 & 0 & 0 \\ -\sin\theta & \cos\theta & 0 & 0 & 0 & 0 \\ 0 & 0 & 1 & 0 & 0 & 0 \\ 0 & 0 & 0 & \cos\theta & \sin\theta & 0 \\ 0 & 0 & 0 & -\sin\theta & \cos\theta & 0 \\ 0 & 0 & 0 & 0 & 0 & 1 \end{bmatrix} \tag{4.40}
$$

4.2.5 Global Matrices

The global matrix is the matrix that defines the system. It is obtained by placing the elementary matrices obtained and translated into global coordinates in the right places. It is denoted by the global mass matrix *M* and the global stiffness matrix *K*. Finally, the problem is solved using the equation below.

$$
M\ddot{x} + Kx = 0 \tag{4.41}
$$

The procedure for adding element matrices to the global matrix is sampled below. Figure 4.8 shows a frame consisting of two finite elements.

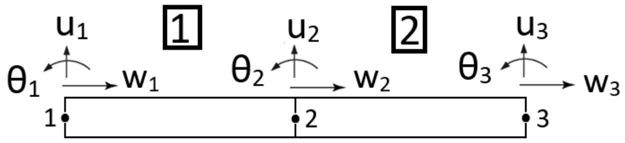

Figure 4.8 A frame element consisting of two elements

Each element shown in Figure 4.9 consists of two nodes and has six degrees of freedom. The node common to the two elements is indicated by the same number.

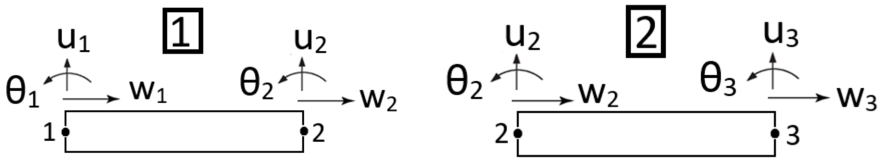

Figure 4.9 Elements of the frame

Equation 4.42 shows the stiffness matrix of each element. The degree of freedom of the elements determines the size of this matrix. Each row and column is numbered. These numbers represent the displacements in the joints.

$$\mathrm{k} = \frac{\rho A l}{420}\begin{array}{c}\begin{matrix} \quad 1 \quad & \quad 2 \quad & \quad 3 \quad & \quad 4 \quad & \quad 5 \quad & \quad 6 \quad \end{matrix} \\ \begin{bmatrix} AE/l & 0 & 0 & -AE/l & 0 & 0 \\ 0 & 12EI/l^3 & 6EI/l^2 & 0 & -12EI/l^3 & -6EI/l^2 \\ 0 & 6EI/l^2 & 4EI/l & 0 & -6EI/l^2 & 2EI/l \\ AE/l & 0 & 0 & AEl & 0 & 0 \\ 0 & 12EI/l^3 & -6EI/l & 0 & 12EI/l^3 & -6EI/l^2 \\ 0 & 6EI/l^2 & 2EI/l & 0 & -6EI/l^2 & 4EI/l \end{bmatrix}\end{array}\begin{matrix} \\ 1 \\ 2 \\ 3 \\ 4 \\ 5 \\ 6 \end{matrix} \qquad (4.42)$$

The size of the global stiffness matrix is the degree of freedom of the entire structure. The stiffness matrix of the element given in Figure 4.8 is given in Equation 4.43. The matrix given in Equation 4.42 is placed in the global stiffness matrix for each element. In the placement process, the displacement number at the joints is taken into account. Each cell in the matrix is placed in the global stiffness matrix according to the row and column number, and the stiffness matrix of the element given in Figure 4.8 is obtained.

As a result, this method is applied to frame structures consisting of many elements to obtain a global stiffness and mass matrix.

$$
\mathrm{k} = \frac{\rho A l}{420}
\begin{array}{c}
\begin{array}{ccccccccc}
1 & 2 & 3 & 4 & 5 & 6 & 7 & 8 & 9
\end{array} \\
\left[\begin{array}{ccccccccc}
AE/l & 0 & 0 & -AE/l & 0 & 0 & 0 & 0 & 0 \\
0 & 12EI/l^3 & 6EI/l^2 & 0 & -12EI/l^3 & -6EI/l^2 & 0 & 0 & 0 \\
0 & 6EI/l^2 & 4EI/l & 0 & -6EI/l^2 & 2EI/l & 0 & 0 & 0 \\
AE/l & 0 & 0 & (AE/l + AE/l) & 0 & 0 & -AE/l & 0 & 0 \\
0 & 12EI/l^3 & -6EI/l & 0 & (12EI/l^3 + 12EI/l^3) & (-6EI/l^2 + 6EI/l^2) & 0 & -12EI/l^3 & -6EI/l^2 \\
0 & 6EI/l^2 & 2EI/l & 0 & (-6EI/l^2 + 6EI/l^2) & (4EI/l + 4EI/l) & 0 & -6EI/l^2 & 2EI/l \\
0 & 0 & 0 & AE/l & 0 & 0 & AE/l & 0 & 0 \\
0 & 0 & 0 & 0 & 12EI/l^3 & -6EI/l & 0 & 12EI/l^3 & -6EI/l^2 \\
0 & 0 & 0 & 0 & 6EI/l^2 & 2EI/l & 0 & -6EI/l^2 & 4EI/l
\end{array}\right]
\end{array}
\begin{array}{c}
\\ 1 \\ 2 \\ 3 \\ 4 \\ 5 \\ 6 \\ 7 \\ 8 \\ 9
\end{array}
\tag{4.43}
$$

4.2.6 Energy Equations for the Spring-Mass System

The suspended mass-spring system with two degrees of freedom with two nodes moving in a single direction used in the study is shown in Figure 4.10.

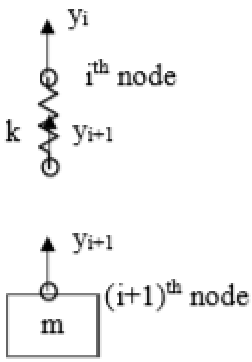

Figure 4.10 The nodes of the suspended mass-spring system

The displacement vector is,

$$q_s{}^T = [\,y_i \quad y_{i+1}] \tag{4.44}$$

The kinetic and potential energy aquations for the mass-spring system is

$$T = \frac{1}{2}\dot{q}_s{}^T m_s \dot{q}_s \tag{4.45}$$

$$U = \frac{1}{2}\dot{q}_s{}^T k_s \dot{q}_s \tag{4.46}$$

m_s is the mass matrix and k_s is the stiffness matrix of the mass-spring system. m_s and k_s are derived from the energy equations and are given below.

$$m_s = m_i \begin{bmatrix} 0 & 0 \\ 0 & 1 \end{bmatrix} \tag{4.47}$$

$$k_s = k_i \begin{bmatrix} 1 & -1 \\ -1 & 1 \end{bmatrix} \tag{4.48}$$

4.2.7 Global Geometric Stiffness Matrix

The geometric stiffness matrix of an element is derived from the strain energy equation. The geometric matrix of the beam element in the frame structure is taken as zero.

$$[K_g]_{beam} = [0] \tag{4.49}$$

$$V = \frac{1}{2} P(t) \int_0^l \left(\frac{du}{dx}\right)^2 dx \tag{4.50}$$

The geometric stiffness matrix (k_g) is obtained by solving Equation (4.50).

$$V = \frac{1}{2} \{u\}^T [k_g] \{u\} \tag{4.51}$$

4.3 Investigation of Dynamic Stability

In the axially loaded system, the matrix-form of motion equation is obtained by substituting the energy equations in the Lagrange equation.

$$M\ddot{q} + K_e q - P(t) K_g q = 0 \tag{4.52}$$

where ,

q is the generalized coordinate

M is the global mass matrix

K_e is the global elastic stiffness matrix

K_g is the global geometric stiffness matrix

P(t) is applied forced.

Equation 4.53 is known as the Mathieu-Hill equation. Periodic distributed dynamic load *P(t)* defined as,

$$P(t) = P_0 + P_t cos\Omega t \tag{4.53}$$

where P_t and P_0 are time depended and static components of load and **Ω** is the disturbing frequency. If the periodic axial load *P(t)* is rewritten related to the static buckling load P_{cr},

$$P(t) = \alpha P_{cr} + \beta P_{cr} cos\Omega t \tag{4.54}$$

where,

$$\alpha = \frac{P_0}{P_{cr}} \tag{4.55}$$

$$\beta = \frac{P_t}{P_{cr}} \tag{4.56}$$

Where α is the static load parameter and β is dynamic load parameter. If Equation 4.54 is put into Equation 4.52, the following equation appears.

$$M\ddot{q} + \left[K_e - \alpha P_{cr} K_{gs} - \beta P_{cr} \cos(\Omega t) K_{gt}\right] q = 0 \tag{4.57}$$

where K_{gs} and K_{gt} geometric matrices reflect effects of static P_0 and time-dependent P_t components of the load, respectively (Bolotin, 1964).

If the static and time-dependent components of the load are applied in the same manner, the K_{gs} and K_{gt} matrices will be equal, $K_{gs} \equiv K_{gt} \equiv K_g$. So Equation 4.57,

$$M\ddot{q} + \left[K_e - \alpha P_{cr} K_g - \beta P_{cr} \cos(\Omega t) K_g\right] q = 0 \tag{4.58}$$

takes the shape.

Also, if $K = K_e - \alpha P_{cr} K_g$ is accepted

$$M\ddot{q} + \left[K - \beta P_{cr} \cos(\Omega t) K_g\right] q = 0 \tag{4.59}$$

is obtained. Equation 4.59 represents a system of second-order differential equation with the periodic coefficient of Mathieu-Hill type.

Equation 4.59 is a periodic function with *T* and *2T* period *(T=2 π /ω)*. The boundaries between stable and unstable regions are created by solutions with T and 2T periods. However, it has been demonstrated by Bolotin that 2T period solutions are the most practical solutions. As a first approach, the dynamic instability boundaries of the main regions are determined from the equation below.

$$\left[K_e - (\alpha \pm \frac{1}{2}\beta) P_{cr} K_g - \frac{\Omega^2}{4} M\right] q = 0 \tag{4.60}$$

Equation (4.60) is solved for the following three situations:

I. Free vibration with ω, in case of $\alpha=0$ and $\beta=0$.

$$[K_e - \omega^2 M]q = 0 \tag{4.61}$$

II. Static stability with $\alpha=1$, $\beta=0$ and $\omega=0$.

$$[K_e - P_{cr}K_g]q = 0 \tag{4.62}$$

III. Dynamic stability in case of the existence of all terms.

$$\left[K_e - (\alpha \pm \frac{1}{2}\beta)P_{cr}K_g - \frac{\Omega^2}{4}M\right]q = 0 \tag{4.63}$$

CHAPTER FIVE

VIBRATION ANALYSIS

5.1 Natural Frequency Analysis

In this study, the problem was solved in MATLAB and ANSYS programs. The results were compared and their accuracy checked. Mode shapes of frame structures were obtained from the ANSYS program. A study was conducted on how many finite elements should be used to obtain the correct solution. The graphic of this study is given in Figure 5.1. As can be seen in Figure 5.1, approximately 20 elements are sufficient to understand the problem. However, the number of the finite elements was selected 60 to suspend the spring-mass system at various points.

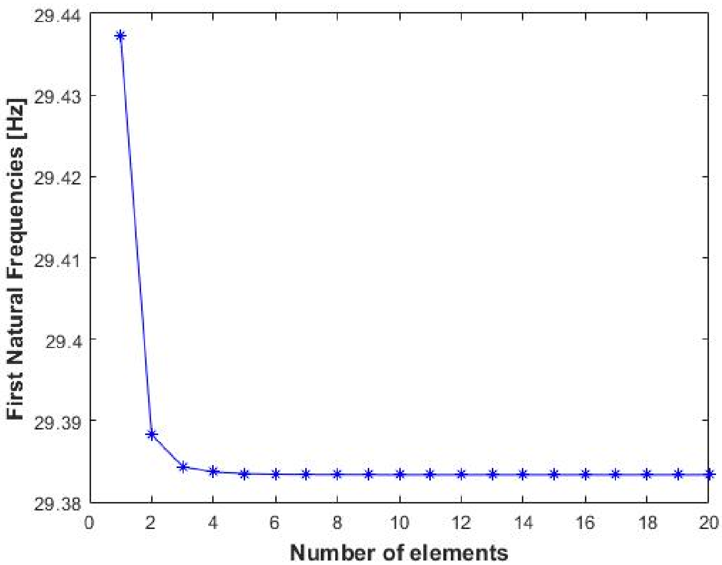

Figure 5.1 Convergence of the frequencies with different number of finite elements

5.2 Natural Frequency Analysis of One-Bay Frame Structure

The model in Thomas, J., Belek, H.T. (1977)'s article was taken as a reference to ensure the accuracy of the analyses. The results are given in Table 5.1. As can be seen from this table, the results are very close.

Table 5.1 The comparison of frequency results between the present model and Thomas, J., Belek, H.T. (1977)'s results

Mode	Frequency (Hz)		
	Thomas, J., Belek, H.T. (1977)	Present Work	
		MATLAB	ANSYS
1	152.7	154.41	154.43
2	604.2	600.91	601.05
3	984.5	974.65	974.89
4	1068.6	1058.72	1059.21

When examining effects of suspended spring-mass systems on frame structures, a one-bay frame will be taken as reference. The dimensions of the one-bay frame structure are given in Figure 4.1. Material properties were taken as $q = 7836.8$ kg/m^3 and $E = 1.9512x10^{11}$. In the modeling of frame structures, the frame element given in Section 4.2.3 is used. The beam54 element was used in the ANSYS program. The beam54 element shows the properties of the frame element.

Figure 5.2 shows the first six mode shapes of the one-bay frame structure.

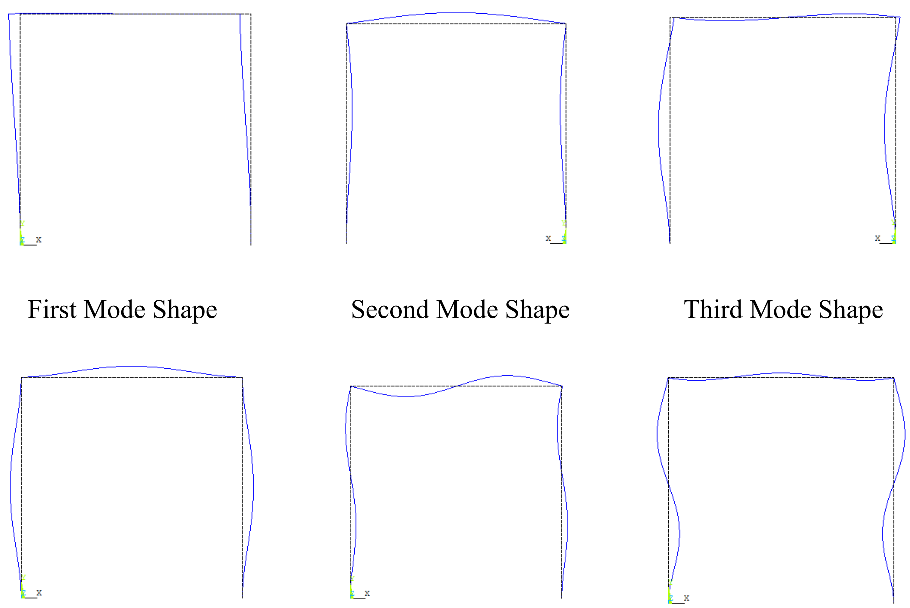

First Mode Shape — Second Mode Shape — Third Mode Shape

Fourt Mode Shape — Fifth Mode Shape — Sixth Mode Shape

Figure 5.2 The first six mode shapes of the one-bay frame structure

Table 5.2 shows the first six natural frequency values of the one-bay frame structure. As can be seen in the table, MATLAB and ANSYS results are the same.

Table 5.2 The comparison of frequency results between MATLAB and ANSYS

Mode	Frequency (Hz)	
	MATLAB	ANSYS
1	29.38	29.39
2	115.90	115.88
3	189.15	189.10
4	204.87	204.83
5	413.33	413.05
6	505.43	505.06

5.3 Effects of Suspended Spring-Mass Systems on Frame Structures

This section shows how the suspended spring-mass systems are hung on frame structures. Spring-mass systems are hung symmetrically on the beam element. Analyses for cases that are not symmetrical are described in the relevant sections. When the single spring-mass element is used, the spring-mass element is hung on the node in the middle of the beam. When more than one element is used, it is hung on the beam at equal intervals. In multi-bay frames, the suspended spring-mass element is hung in each compartment equally and symmetrically. These situations are shown in Figure 5.3 and Figure 5.4.

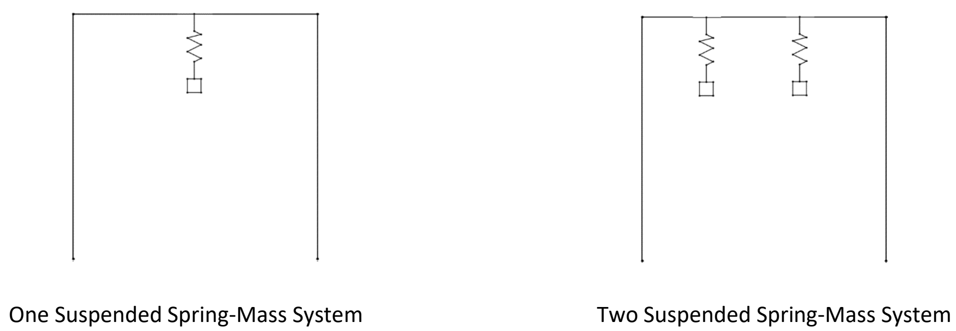

Figure 5.3 One-bay frame structure with one and two suspended spring-mass systems

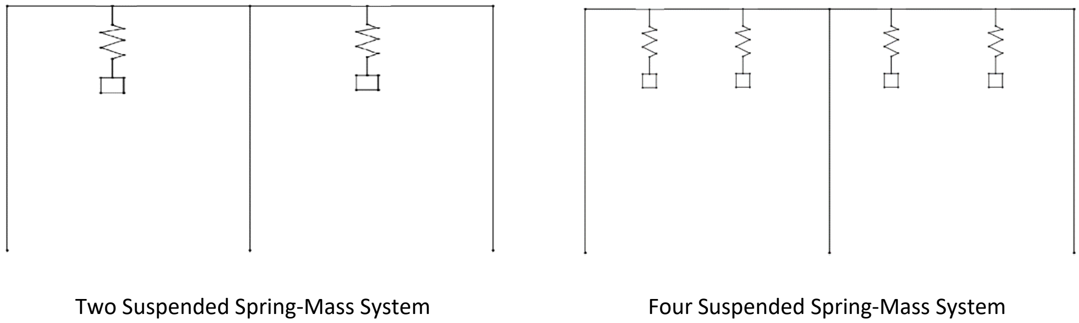

Figure 5.4 The two-bay fame structure with two and four suspended spring-mass systems

Analyzes are made for three different spring stiffness coefficients of the suspended spring-mass system. These values are $k_{s1} = 10000\ N/m$, $k_{s2} = 65000\ N/m$ and $k_{s3} = 1000000\ N/m$. The frequency value of the suspended spring-mass system for k_{s1} is 11.25 Hz. This value is much smaller than the first frequency value of the frame system. When k_{s2} is used, the frequency value is 28.69 Hz. This value is close to the first frequency value of the frame system. In k_{s3}, the frequency value is 112.54 and it is greater than the first frequency value of the frame system and smaller than the second frequency value.

5.3.1 Effects of Suspended Spring-Mass Systems on One-bay Frame Structure

In this section, effects of suspended spring-mass systems on the natural frequency and mode shapes of one-bay frame systems are examined.

The mode shapes of the one-bay frame system with the single suspended spring-mass system for k_{s1} are given in Figure 5.5.

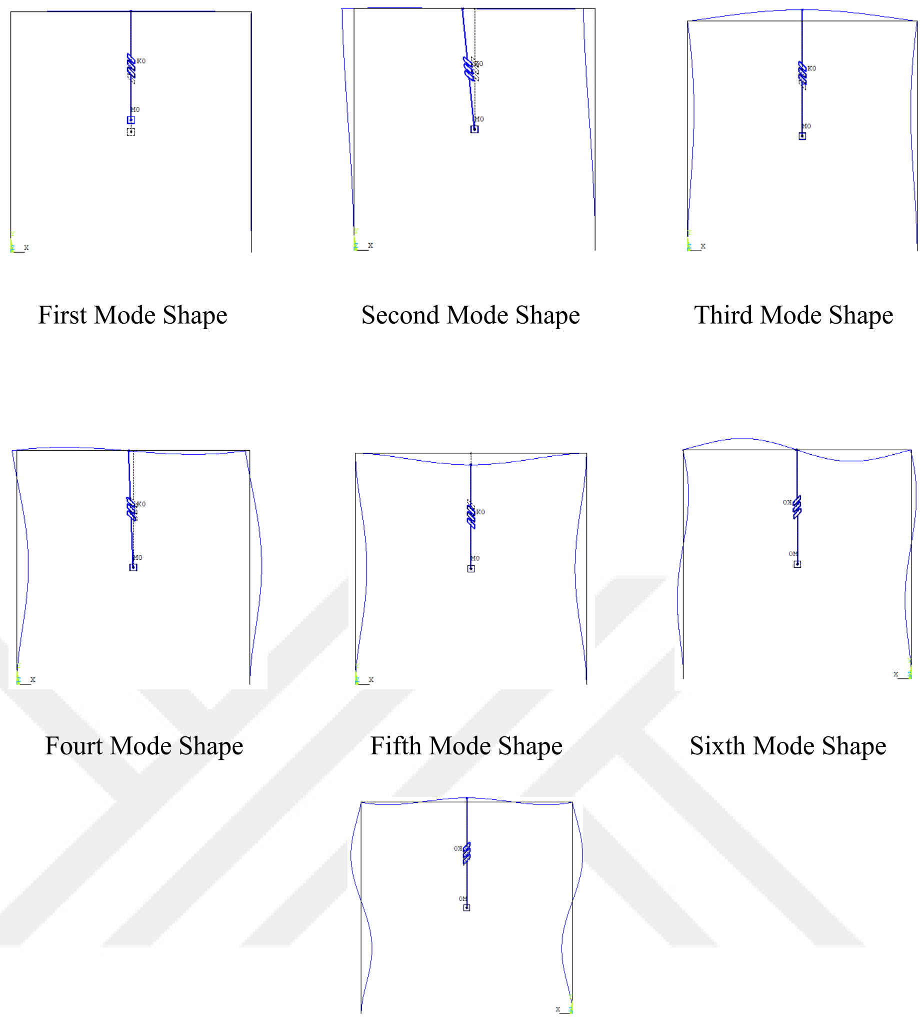

First Mode Shape   Second Mode Shape   Third Mode Shape

Fourt Mode Shape   Fifth Mode Shape   Sixth Mode Shape

Seventh Mode Shape

Figure 5.5 The first seven mode shapes of the one-bay frame structure with one suspended spring-mass system with k_{s1}

Comparing Figure 5.5 with Figure 5.2:

- In the first mode shape given in Figure 5.5, it is seen that the suspended spring-mass system is dominant. There is no significant displacement in the frame system.
- It is seen that other mode shapes are almost the same as those given in Figure 5.5.

- In this case, it can be said that the first mode shape belongs to the suspended spring-mass system and the natural frequency value of the frame increases by one in the same frequency range.

The mode shapes of the one-bay frame system with single suspended spring-mass system for k_{s2} are given in Figure 5.6.

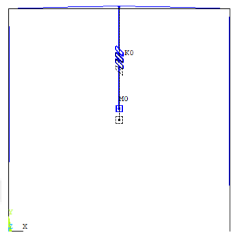

First Mode Shape

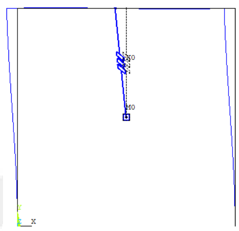

Second Mode Shape

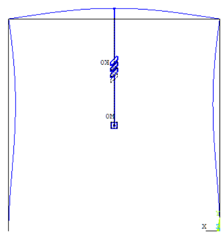

Third Mode Shape

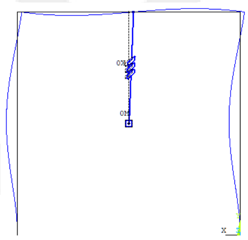

Fourt Mode Shape

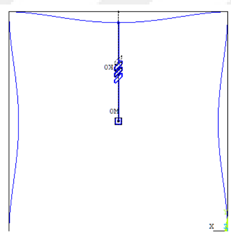

Fifth Mode Shape

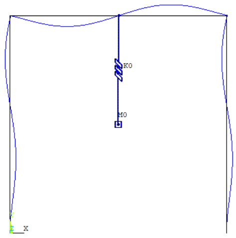

Sixth Mode Shape

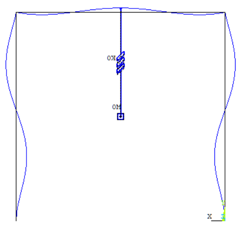

Seventh Mode Shape

Figure 5.6 The first seven mode shapes of the one-bay frame structure with one suspended spring-mass system with k_{s2}

Comparing Figure 5.6 with Figure 5.2 and Figure 5.5 :

- It is seen that the mode shapes given in Figure 5.7 are very similar to those given in Figure 5.6. Therefore, the same evaluations apply to this situation.

The mode shapes of the one-bay frame system with a single suspended spring-mass system for k_{s3} are given in Figure 5.7.

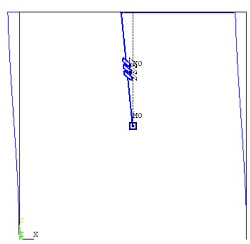

First Mode Shape

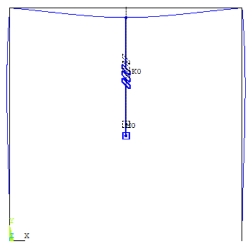

Second Mode Shape

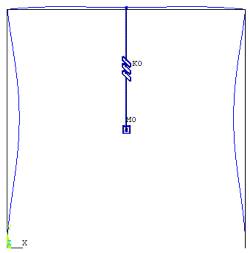

Third Mode Shape

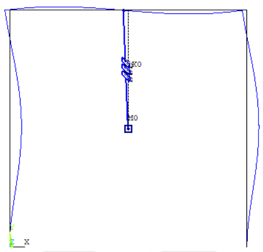

Fourt Mode Shape

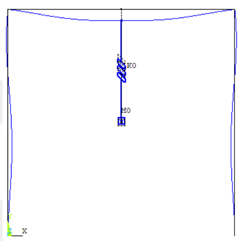

Fifth Mode Shape

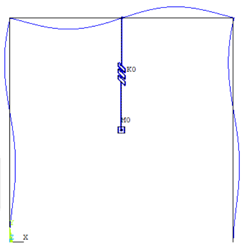

Sixth Mode Shape

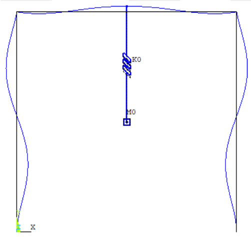

Seventh Mode Shape

Figure 5.7 The first seven mode shapes of the one-bay frame structure with one suspended spring-mass system with k_{s3}

Comparing Figure 5.7 with Figure 5.2, Figure 5.5 and Figure 5.6:

- When the mode shapes given in Figure 5.7 are analyzed, it is seen that there is no mode shapes in which only the suspended spring-mass system is dominant. Beam and suspended spring-mass systems move together, as in the second form of vibration. It can be said that the second mode shape is due to the suspended spring-mass system. Because the frequency value of the suspended spring-mass system is between the first and second frequency values of the frame in Figure 5.5.

- It is seen that the suspended spring-mass system has no effect on the first mode shape. In this mode shape, the column element is dominant and there is no vertical displacement.
- The sixth mode shape is the same as the fifth mode shape in Figure 5.2 and the sixth mode shape in Figure 5.5. Looking at Table 5.3, it is seen that the frequency values are the same. Also in this form of vibration, the point where the suspended spring-mass system hangs is displaced. This explains why the suspended spring-mass system does not affect the frame system.

The frequency values of the one-bay frame system with a single suspended spring-mass system for k_{s1}, k_{s2} and k_{s3} are given in Table 5.3.

Table 5.3 The first seven frequency values of the one-bay frame structure with one suspended spring-mass system with k_{s1}, k_{s2} and k_{s3}

Mode	Frequency (Hz)		
	k_{s1}	k_{s2}	k_{s3}
1	11.03	25.44	29.38
2	29.38	29.38	47.160
3	117.75	127.33	170.74
4	189.10	189.15	189.10
5	205.50	209.60	313.29
6	413.05	413.33	413.05
7	505.11	505.80	512.28

The mode shapes of the one-bay frame system with two suspended spring-mass system for k_{s1} are given in Figure 5.8.

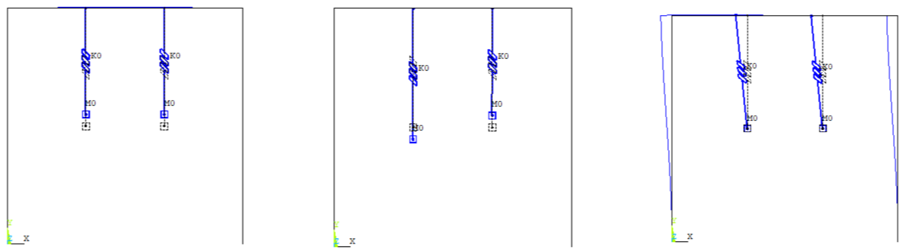

First Mode Shape Second Mode Shape Third Mode Shape

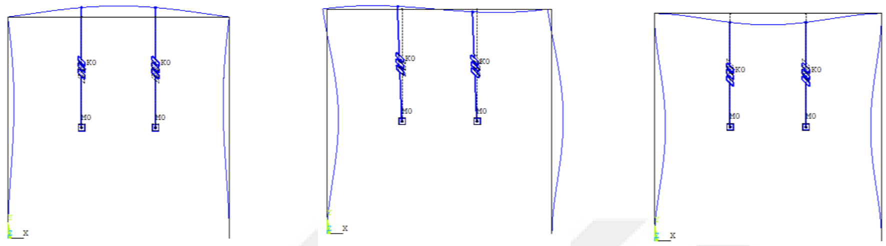

Fourt Mode Shape Fifth Mode Shape Sixth Mode Shape

Seventh Mode Shape Eighth Mode Shape

Figure 5.8 The first eight mode shapes of the one-bay frame structure with two suspended spring-mass systems with k_{s1}

Comparing Figure 5.8 with Figure 5.2, Figure 5.5:

- It is seen that the natural frequency response in the same frequency range increased by one compared to Figure 5.5.
- It is seen that the first two mode shapes belong to the suspended spring-mass system. It is seen that the other mode shapes are the same as the mode shapes given in Figure 5.2.
- In this case, it has been understood that suspended spring-mass systems for k_{s1} do not change the basic mode shapes of the frame structures, but create a new natural frequency response as much as the number of suspended mass springs.

The mode shapes of the one-bay frame system with two suspended spring-mass system for k_{s2} are given in Figure 5.9.

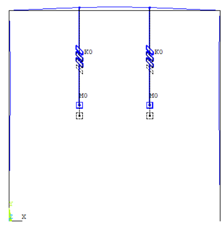

First Mode Shape

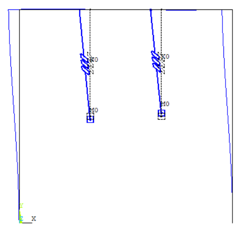

Second Mode Shape

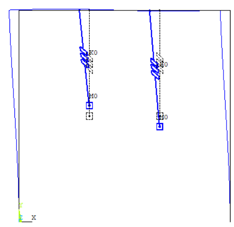

Third Mode Shape

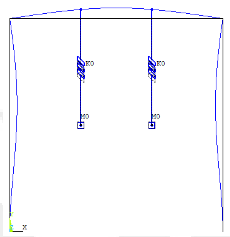

Fourt Mode Shape

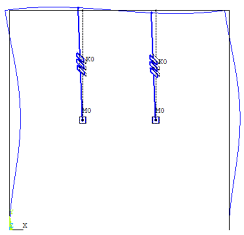

Fifth Mode Shape

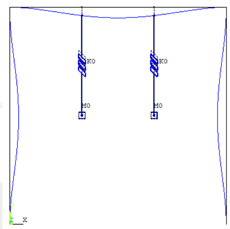

Sixth Mode Shape

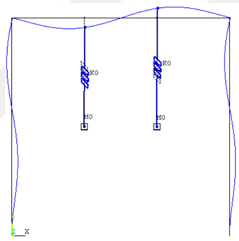

Seventh Mode Shape

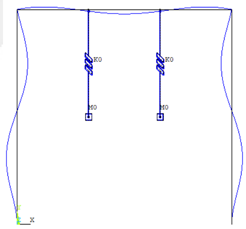

Eighth Mode Shape

Figure 5.9 The first eight mode shapes of the one-bay frame structure with two suspended spring-mass systems with k_{s2}

Comparing Figure 5.9 with Figure 5.2, Figure 5.6 and 5.8:

- It is seen that the mode shapes given in Figure 5.9 are very similar to those given in Figure 5.8. Therefore, the same evaluations apply to this situation.
- As the only difference is that the number of suspended spring-mass is two, two new mode shapes have occurred.

The mode shapes of the one-bay frame system with two suspended spring-mass system for k_{s3} are given in Figure 5.10.

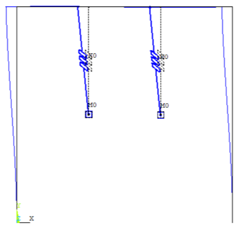

First Mode Shape

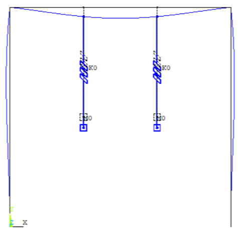

Second Mode Shape

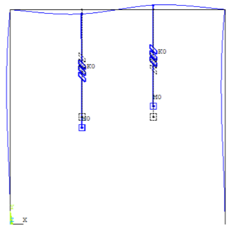

Third Mode Shape

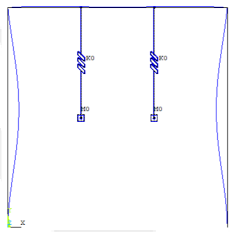

Fourt Mode Shape

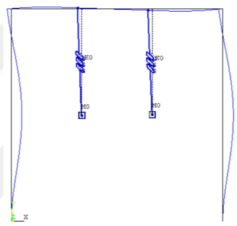

Fifth Mode Shape

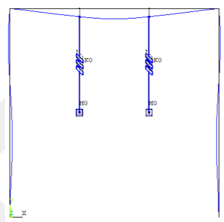

Sixth Mode Shape

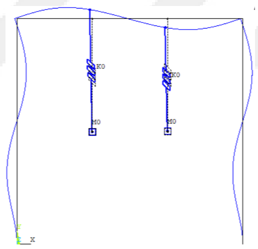

Seventh Mode Shape

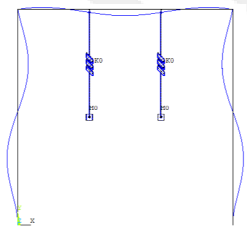

Eighth Mode Shape

Figure 5.10 The first eight mode shapes of the one-bay frame structure with two suspended spring-mass systems with k_{s3}

Comparing Figure 5.10 with Figure 5.2, Figure 5.7, Figure 5.8 and Figure 5.9:

- When the mode shapes given in Figure 5.10 are examined, it is observed that similar results are seen in Figure 5.7.
- Two new mode shapes appear in the same frequency band, and these are the second and third mode shapes. These mode shapes are caused by the suspended spring-mass system. The reason for occurrence in this range is that the

frequency value of the suspended spring-mass system is between the first and second frequency value of the one-bay frame in Figure 5.2.

- The only effect of the number of suspended spring-mass systems on frame systems is that it creates a new mode shape as much as the number of suspended spring-mass in the same frequency band.

The frequency values of the one-bay frame system with two suspended spring-mass systems for k_{s1}, k_{s2} and k_{s3} are given in Table 5.4.

Table 5.4 The first eight frequency values of the one-bay frame structure with two suspended spring-mass system with k_{s1}, k_{s2} and k_{s3}

Mode	Frequency (Hz)		
	k_{s1}	k_{s2}	k_{s3}
1	10.95	24.46	29.29
2	11.21	27.55	41.69
3	29.39	29.96	86.17
4	118.58	131.92	176.07
5	189.20	189.80	196.50
6	205.64	210.89	356.94
7	413.89	418.74	474.51
8	505.07	505.54	508.01

5.3.2 Effects of Suspended Spring-Mass Systems on the Two-Bay Frame Structures

In this section, effects of suspended spring-mass systems on the natural frequency and mode shapes of the two-bay frame systems are examined. As it is done in Chapter 5.3.1, first the mode shapes and natural frequencies of the two-bay frame without suspended spring-mass are given and effects of the hanging spring-mass systems have been investigated by using these results.

Figure 5.11 shows the first nine mode shapes of the two-bay frame.

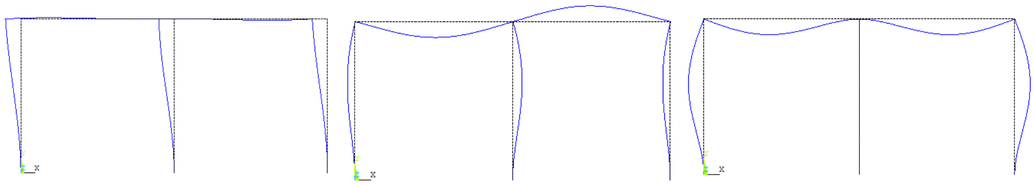

First Mode Shape Second Mode Shape Third Mode Shape

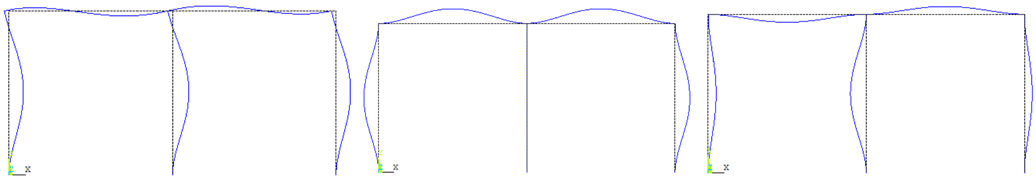

Fourt Mode Shape Fifth Mode Shape Sixth Mode Shape

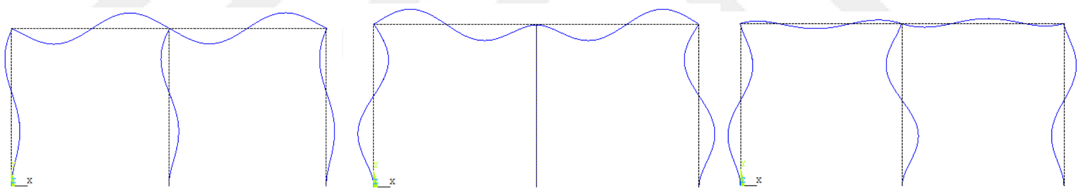

Seventh Mode Shape Eighth Mode Shape Ninth Mode Shape

Figure 5.11 The first nine mode shapes of the two-bay frame structure

Table 5.5 shows the first nine frequency values of the two-bay frame structure

Table 5.5 The first nine frequency volues of the two-bay frame structure

Mode	Frequency (Hz)
1	27.23
2	112.09
3	141.14
4	190.40
5	204.53
6	204.97
7	405.40
8	455.46
9	514.29

When Table 5.5, Table 5.2 and Figure 5.2, Figure 5.11 are compared, it is seen that there are more natural frequency responses in the same frequency band compared to the one-bay frame. This is because the number of some modes increases as the number of bays increases. This situation was explained by Erkan, Öztürk and Sabuncu (2013). The third, fifth and eighth modes in the table are modes created in this way. This must be taken into account when examining effects of suspended spring-mass systems on the two-bay frames.

The mode shapes of the two-bay frame system with two suspended spring-mass system for k_{s1} are given in Figure 5.12.

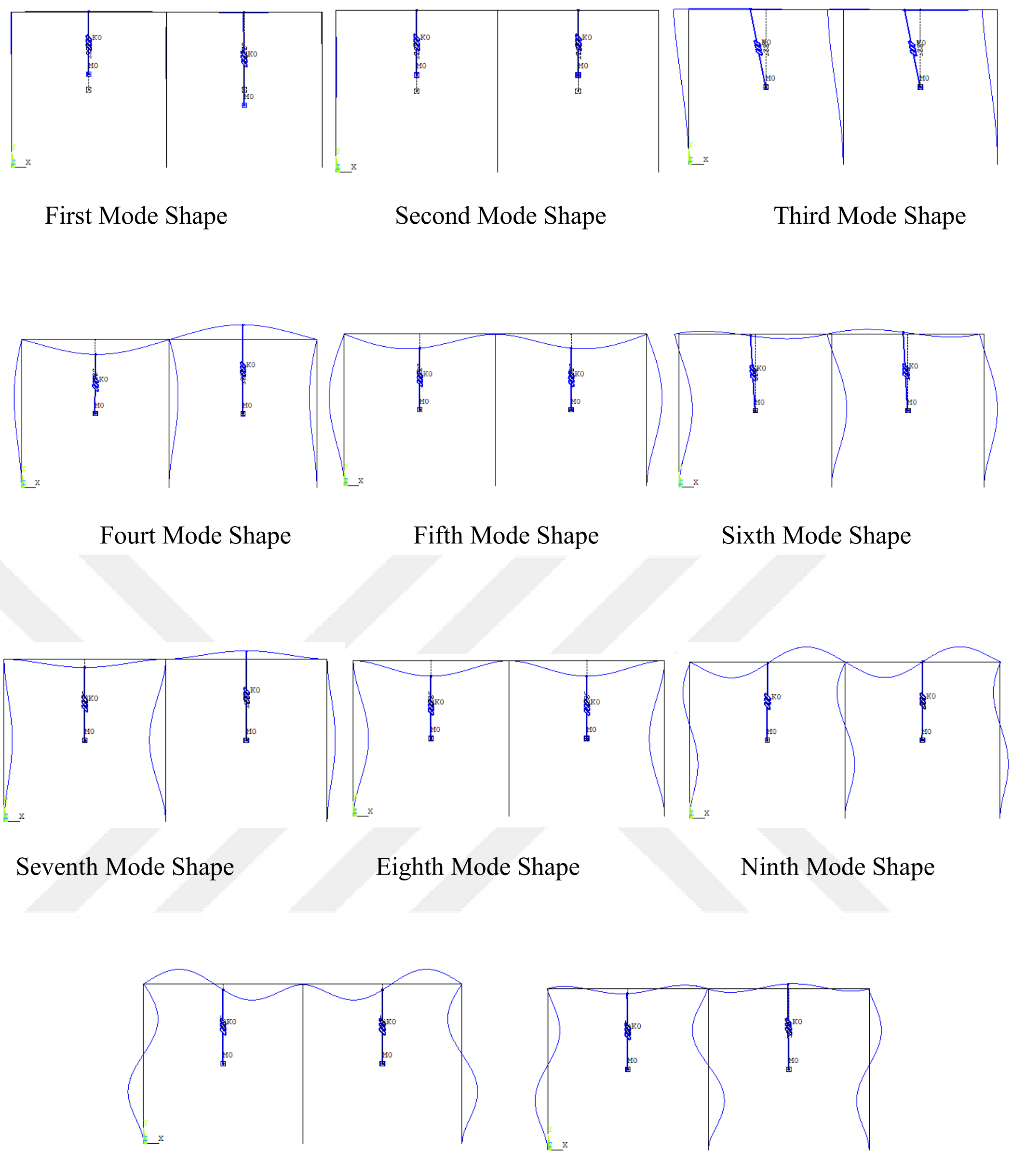

First Mode Shape Second Mode Shape Third Mode Shape

Fourt Mode Shape Fifth Mode Shape Sixth Mode Shape

Seventh Mode Shape Eighth Mode Shape Ninth Mode Shape

Tenth Mode Shape Eleventh Mode Shape

Figure 5.12 The first nine mode shapes of the two-bay frame structure with two suspended spring-mass systems with k_{s1}

Comparing Figure 5.12 with Figure 5.11:

- It is seen in Figure 5.12 that the suspended spring-mass system is dominant in the first and second mode shapes.
- The other mode shapes are almost the same as those given in Figure 5.12.

- For the k_{s1} value, it is understood that the one-bay frame with a hanging spring-mass system given in Figure 5.5 and the frame system whose results are given in Figure 5.12 show similar behavior.

The mode shapes of the two-bay frame system with two suspended spring-mass system for k_{s2} are given in Figure 5.13.

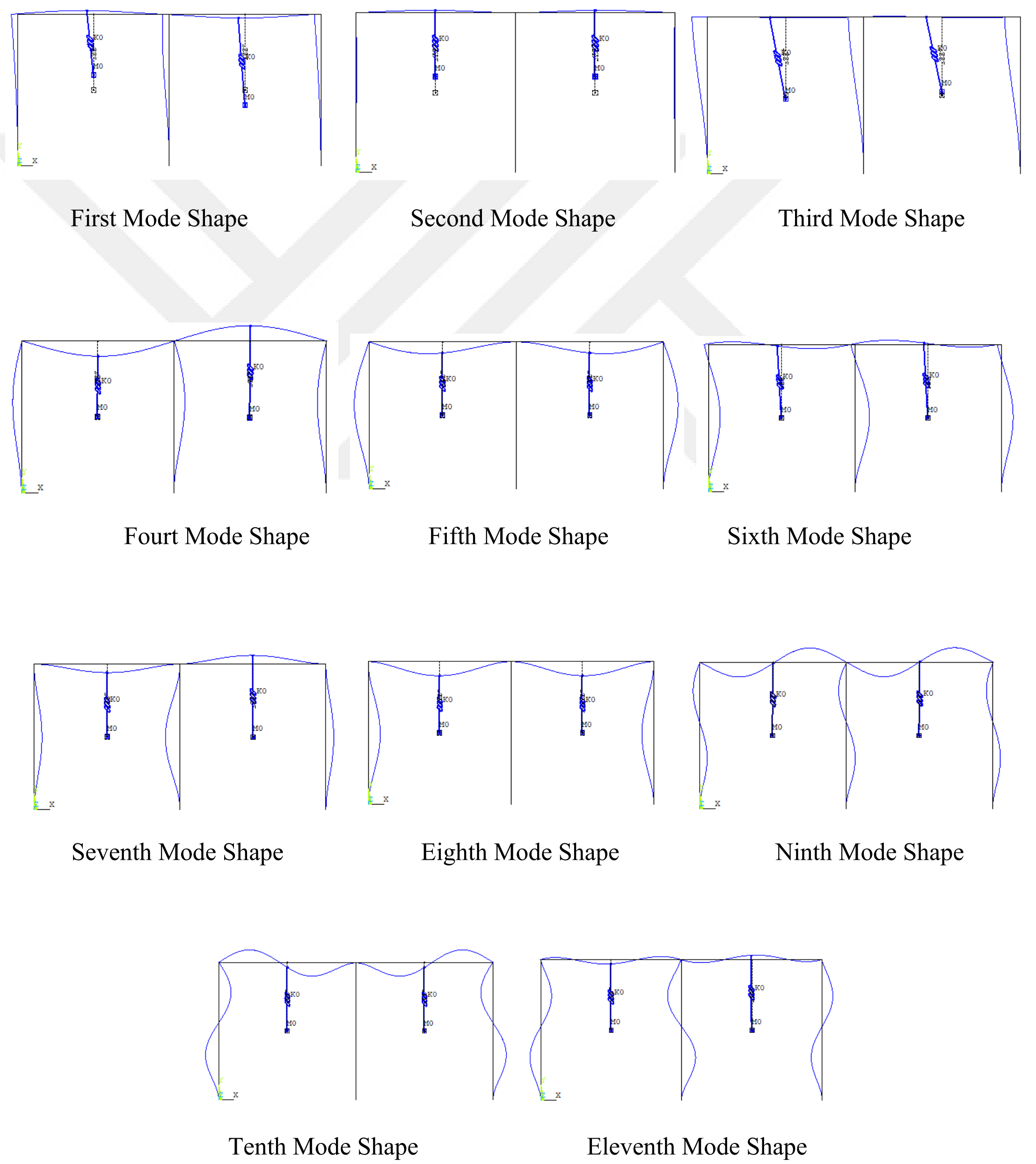

Figure 5.13 The first nine mode shapes of the two-bay frame structure with two suspended spring-mass systems with k_{s2}

Comparing Figure 5.13 with Figure 5.12 and Figure 5.11 :

- It is seen that the mode shapes given in Figure 5.12 are very similar to those given in Figure 5.13. Therefore, the evaluation made for the mode shapes given in Figure 5.12 is also valid for the mode shapes given in Figure 5.13. Likewise, in the comparison of Figure 5.6 and Figure 5.5, it is seen that there was no difference between the mode shapes.

The mode shapes of the two-bay frame system with two suspended spring-mass system for k_{s3} are given in Figure 5.14.

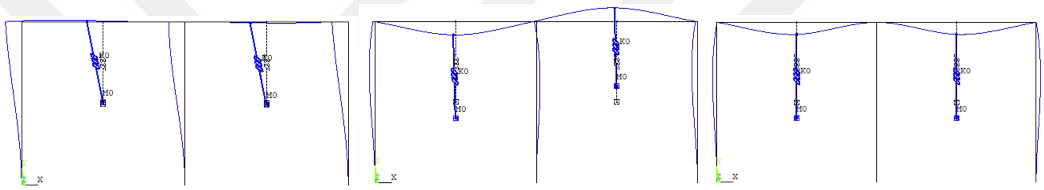

First Mode Shape Second Mode Shape Third Mode Shape

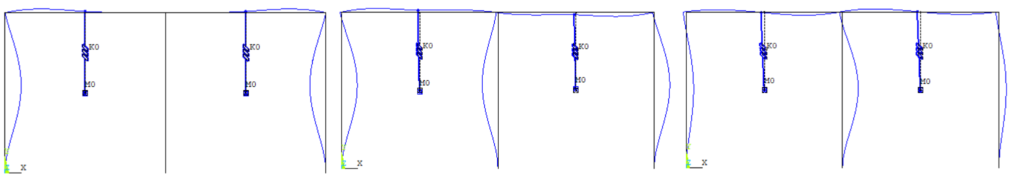

Fourt Mode Shape Fifth Mode Shape Sixth Mode Shape

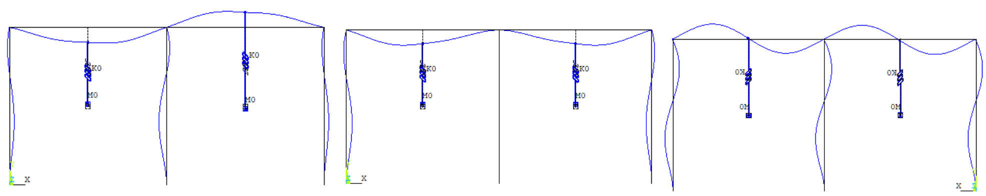

Seventh Mode Shape Eighth Mode Shape Ninth Mode Shape

Figure 5.14 The first nine mode shapes of the two-bay frame structure with two suspended spring-mass systems with k_{s3}

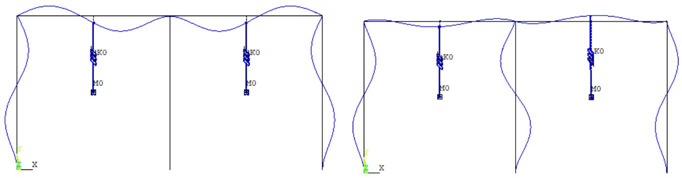

Tenth Mode Shape Eleventh Mode Shape

Figure 5.14 continues

Comparing Figure 5.14 with Figure 5.11, Figure 5.12 and Figure 5.13:

- When the mode shapes given in Figure 5.14 are examined, it is seen that there is no mode shape dominated by only the suspended spring-mass system. When the second and third mode shapes are examined, it is understood that these mode shapes act together with the beam and the suspended spring-mass system. The fact that the frequency value of the suspended spring mass system is between the first and the second frequency values of the frame system supports this result.
- The suspended spring-mass system has no effect on the first mode shapes.
- It can be seen that other mode shapes are similar to those given in Figure 5.11-5.12-5.13. However, it is also understood that the displacements occurring in the beam element slightly differentiated and the vibration frequencies increased. As a result, it can be said that the main characteristics of the frequency ranges and mode shapes do not change.

The frequency values of the two-bay frame system with two suspended spring-mass systems for k_{s1}, k_{s2} and k_{s3} are given in Table 5.6.

Table 5.6 The first eleven frequency values of the two-bay frame structure with two suspended spring-mass system with k_{s1}, k_{s2} and k_{s3}

Mode	Frequency (Hz)		
	k_{s1}	k_{s2}	k_{s3}
1	11.00	24.85	27.136
2	11.10	26.36	45.207
3	27.236	27.52	55.254
4	114.24	125.28	169.95
5	142.32	148.09	175.58
6	190.41	190.56	191.17
7	205.48	208.64	306.91
8	205.53	211.58	326.84
9	405.40	405.68	405.64
10	455.35	426.15	464.12
11	514.35	515.05	521.23

When comparing Table 5.6 with Table 5.3:

- The first two frequency values given for k_{s1} and k_{s2} belong to the suspended spring-mass system. The second and third frequency values obtained for k_{s3} belong to the suspended spring-mass system.
- Thus, it has been observed that the increase in the number the frame does not change the results described above.

The mode shapes of the two-bay frame system with four suspended spring-mass system for k_{s1} are given in Figure 5.15.

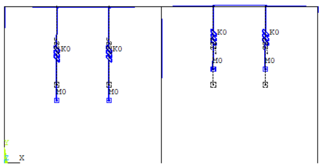

First Mode Shape

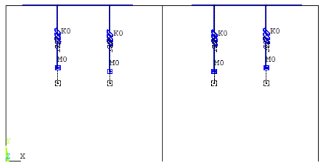

Second Mode Shape

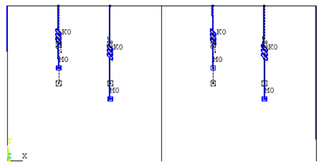

Third Mode Shape

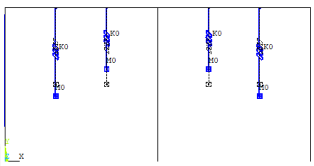

Fourt Mode Shape

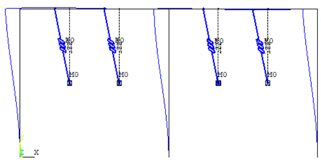

Fifth Mode Shape

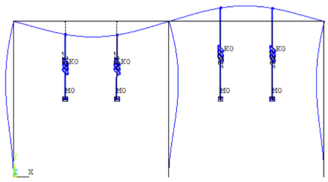

Sixth Mode Shape

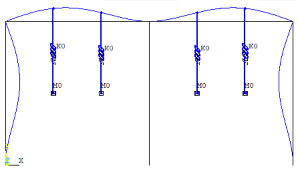

Seventh Mode Shape

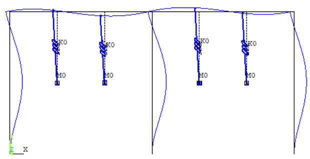

Eighth Mode Shape

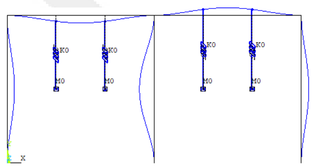

Ninth Mode Shape

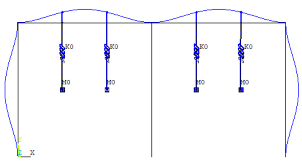

Tenth Mode Shape

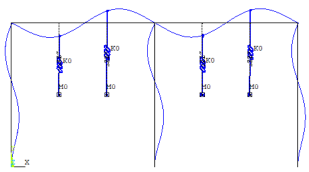

Eleventh Mode Shape

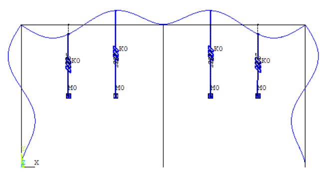

Twelfth Mode Shape

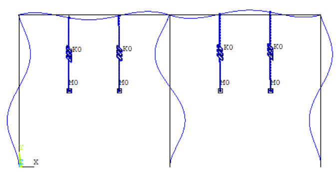

Thirteenth Mode Shape

Figure 5.15 The first nine mode shapes of the two-bay frame structure with four suspended spring-mass systems with k_{s1}

The mode shapes of the two-bay frame system with four suspended spring-mass system for k_{s2} are given in Figure 5.16.

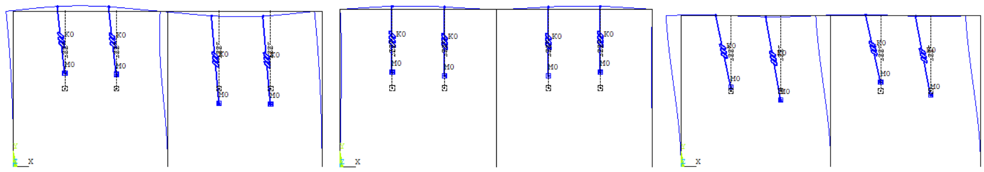

First Mode Shape Second Mode Shape Third Mode Shape

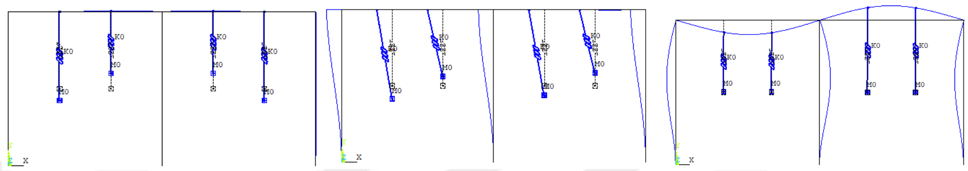

Fourt Mode Shape Fifth Mode Shape Sixth Mode Shape

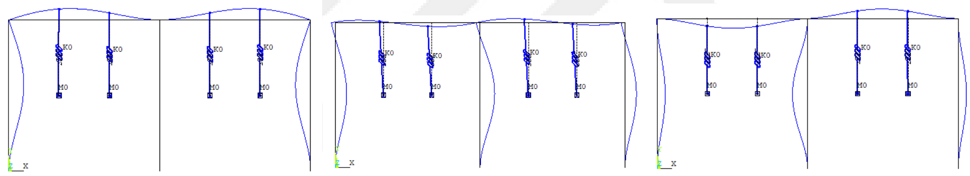

Seventh Mode Shape Eighth Mode Shape Ninth Mode Shape

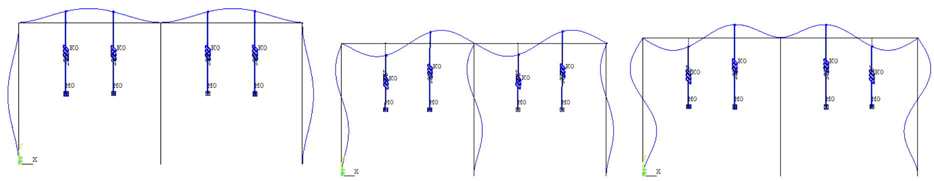

Tenth Mode Shape Eleventh Mode Shape Twelfth Mode Shape

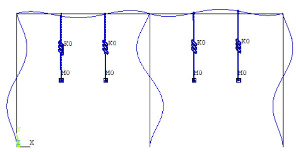

Thirteenth Mode Shape

Figure 5.16 The first nine mode shapes of the two-bay frame structure with four suspended spring-mass systems with k_{s2}

The mode shapes of the two-bay frame system with four suspended spring-mass system for k_{s3} are given in Figure 5.17.

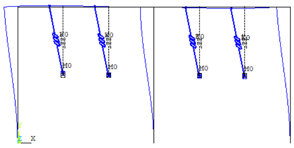

First Mode Shape

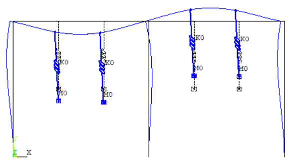

Second Mode Shape

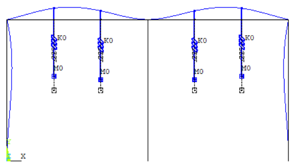

Third Mode Shape

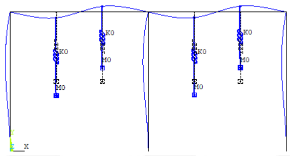

Fourt Mode Shape

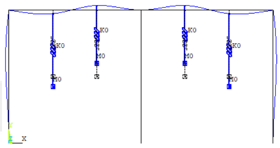

Fifth Mode Shape

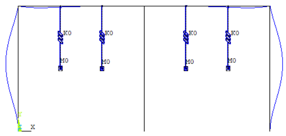

Sixth Mode Shape

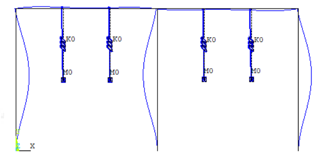

Seventh Mode Shape

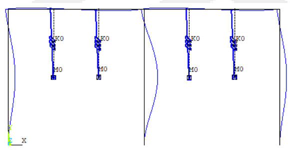

Eighth Mode Shape

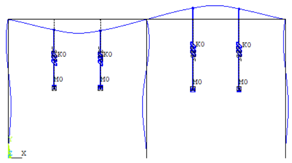

Ninth Mode Shape

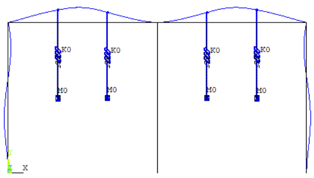

Tenth Mode Shape

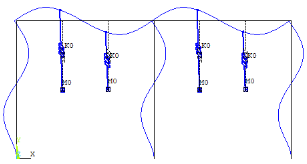

Eleventh Mode Shape

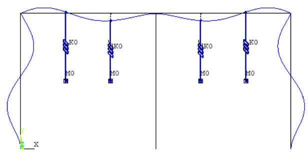

Twelfth Mode Shape

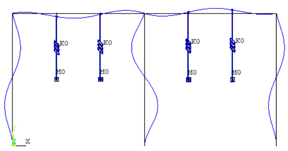

Thirteenth Mode Shape

Figure 5.17 The first nine mode shapes of the two-bay frame structure with four suspended spring-mass systems with k_{s3}

The frequency values of the two-bay frame system with four suspended spring-mass systems for k_{s1}, k_{s2} and k_{s3} are given in Table 5.7.

Table 5.7 The first thirteen frequency values of the two-bay frame structure with four suspended spring-mass system with k_{s1}, k_{s2} and k_{s3}

Mode	Frequency (Hz)		
	k_{s1}	k_{s2}	k_{s3}
1	10.91	23.77	27.01
2	11.05	25.74	39.76
3	11.21	26.91	50.05
4	11.23	28.21	85.60
5	27.25	28.71	90.38
6	115.20	130.65	175.67
7	142.84	150.84	181.08
8	190.52	191.23	197.88
9	205.59	209.67	353.56
10	205.75	213.40	367.05
11	406.31	411.51	473.00
12	456.05	459.49	489.02
13	514.32	514.82	517.72

Figure 5.15, Figure 5.16, Figure 5.17 and Table 5.7 show, the results of the two-bay frame system with four suspended spring-mass systems for values k_{s1}, k_{s2} and k_{s3}. When these results are examined;

- As seen in Table 5.7, new natural frequencies have been formed as much as the number of suspended spring-mass systems.
- In the analysis for the k_{s1} and k_{s2} values, it was seen that the new modes added to the frame structure appeared as the first modes and had no effect on the other modes

- In the analysis for the ks3 value, it is seen that the new modes added to the frame system occur between the first and second modes of the frame system.
- As a result, similar results were observed with the two-bay frame system with two suspended spring-mass systems.

5.3.3 Effects of Asymmetrically Suspended Spring-Mass Systems on Frame Structures

Another analysis was made for the case when the suspended spring-mass system was asymmetrically hung on the frame system. The spring-mass system is located in the *L/3* position of the beam element.

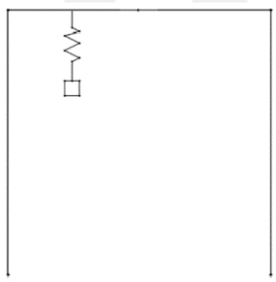

Figure 5.18 The one-bay frame structure with asymmetric one suspended spring-mass system

Free vibration frequencies are given in Table 5.8.

Table 5.8 The first seven frequency values of the one-bay frame structure with one asymmetric suspended spring-mass system with k_{s1}, k_{s2} and k_{s3}

Mode	Frequency (Hz)		
	k_{s1}	k_{s2}	k_{s3}
1	11.08	25.95	29.33
2	29.39	29.51	51.82
3	117.26	124.38	165.99
4	189.20	189.46	191.09
5	205.27	207.68	261.39
6	413.76	416.12	459.60
7	505.44	505.49	506.88

Comparing Table 5.8 to Table 5.3:

- It has been observed that frequency values are almost unchanged for k_{s1} and k_{s2}.
- In the results given for k_{s3}, it was seen that the biggest change was in the fifth frequency value. The reason for this situation is that in case of symmetrical loading, the spring-mass system corresponds to the node that there is no vertical movement in this form of vibration, but this is not the case in asymmetrical loading.
- As a result, it was determined that the results obtained in the case of asymmetric suspending of the spring-mass systems to the frame structures are not different from the results obtained in the case of symmetrical suspending.

CHAPTER SIX

DYNAMIC STABILITY ANALYSIS

The dynamic stability analysis of frame structures was performed for different numbers of frames, suspended spring-mass, and different suspended spring-mass stiffness coefficients. In addition, the asymmetric suspend of the mass-spring system to the frame system was also examined. The obtained results were given in graphics and the results were interpreted.

In order to validate the analysis model, the critical buckling load for different bay numbers was calculated in MATLAB and ANSYS programs. The results obtained are given in Table 6.1. When Table 6.1 is examined, it is seen that the results are very close.

Table 6.1 Comparison of critical buckling load values obtained from present work and ANSYS program for different bay numbers

Number of bay	Critical buckling load parameters	
	Present Work	ANSYS
1	74165	74142.8
2	76462	76443.24
3	78754	78742.38
4	79935	79928.12
5	80751	80748.54

6.1 Effect of Number of Bay

Effect of the number of the bay and the dynamic stability parameter (β) on dynamic stability regions are given in Figures 6.1-6.4. The charts were created for cases where the number of bays is one, two, three, four, and five and the static load parameter is zero and 0.5. The horizontal axis of the graph shows the dynamic load parameter and the vertical axis shows the ratio of the disturbing frequency (Ω_1-Ω_2) to the first natural frequency of the frame structure with no suspending spring-mass system (ω_1).

Figures 6.1 and 6.2 show the first and second instability regions for the case where the static load coefficient is zero. Figures 6.3 and 6.4 show the instability regions for the case where the static load coefficient is 0.5.

When Figure 6.1 is examined, it is seen that the increase in the number of bays changes the dynamic instability region, but the change is less. It can be understood that this change is more in the second instability region given in Figure 6.2. In addition, it is seen that the second instability region is narrower than the first instability region.

In the case where the static load parameter is 0.5, the dynamic load parameter was limited between zero and one. It was found that the value of the frequency rates decreased and the instability region narrowed.

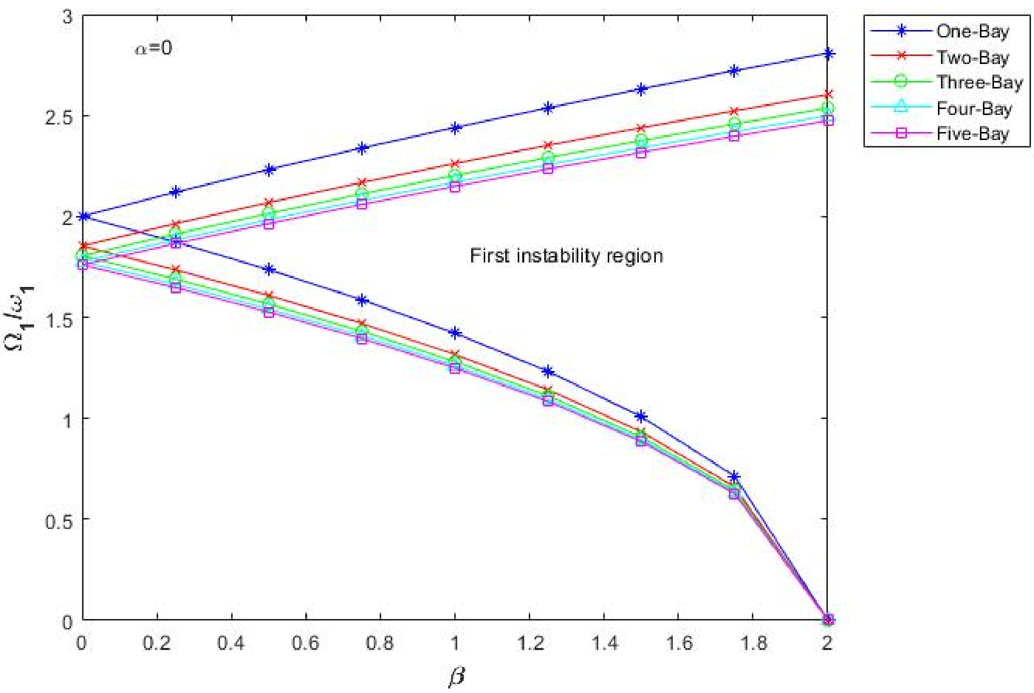

Figure 6.1 Effects of the number of bays on the first stability regions of frame structures, α=0

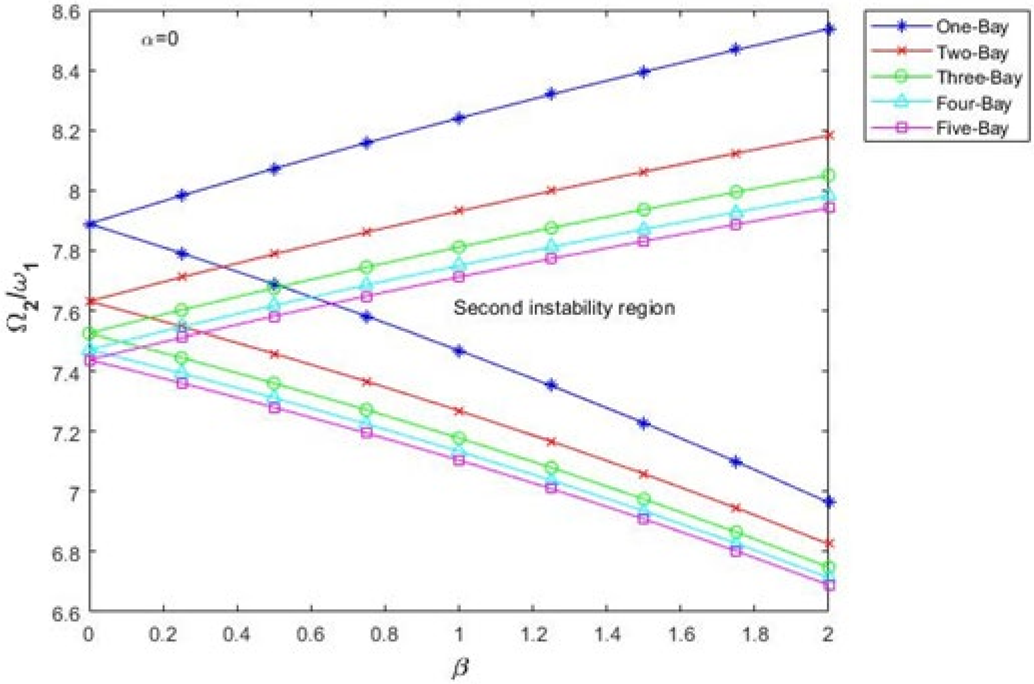

Figure 6.2 Effects of the number of bays on the second stability regions of frame structures, α=0

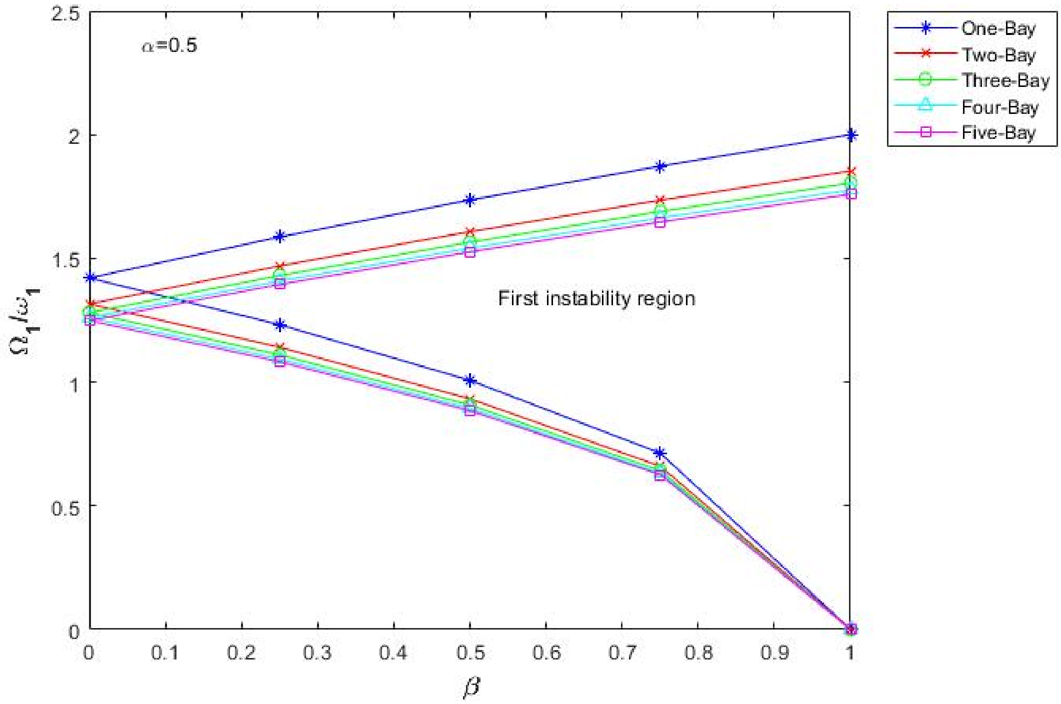

Figure 6.3 Effects of the number of bays on the first stability regions of frame structures, α=0.5

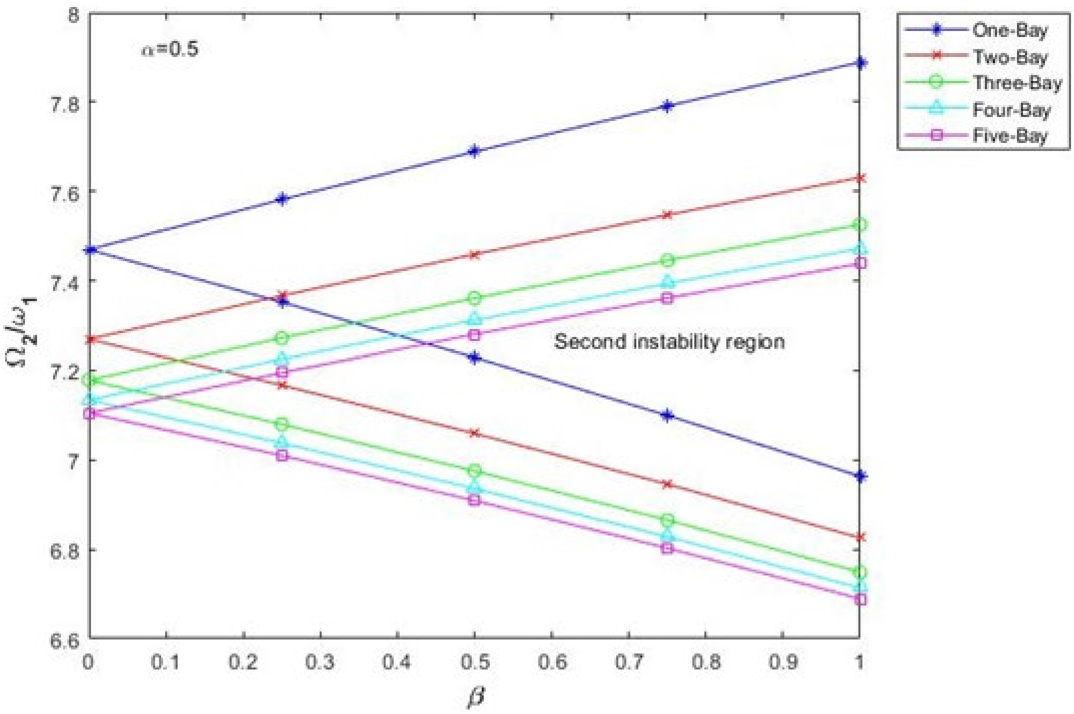

Figure 6.4 Effects of the number of bays on the second stability regions of frame structures, α=0.5

6.2 Effects of the Number and Stiffness Coefficient of Suspended Spring-Mass System on One-Bay Frame Structure

In this section, effects of the number of suspended spring-mass systems and the stiffness coefficient on the dynamic stability regions of single-section frames are examined. In all graphs, the change in the stiffness coefficient of the suspended spring-mass system is represented by k_r. k_r is the ratio of the stiffness coefficient of the suspended spring-mass system to the equivalent stiffness coefficient of the frame structure. The equivalent stiffness coefficient of the frame structure has been calculated from the equation $\omega_n{}^2 = k/m$. In the equation, m is the equivalent mass of the frame structure, and ω_n is the first natural frequency value.

Figures 6.5- 6.8 shows effects of the frame structure of the single-suspended spring-mass system on the dynamic stability region. Figures 6.5 and 6.6 show the first and second regions of instability in the absence of static loading. Figures 6.3 and 6.4 show the regions of instability for static loading.

When Figure 6.1 and Figure 6.5 are compared, it is seen that the first dynamic instability region contracts depending on the k_r value. It was found that the narrowing in the dynamic instability region increased as k_r decreased. When Figure 6.2 and Figure 6.6 are compared, it was seen that the dynamic instability region narrowed. However, it was noticed that the higher the k_r value, the greater the narrowing in the dynamic stability region. Similar results were observed when Figure 6.7 and Figure 6.8 were examined.

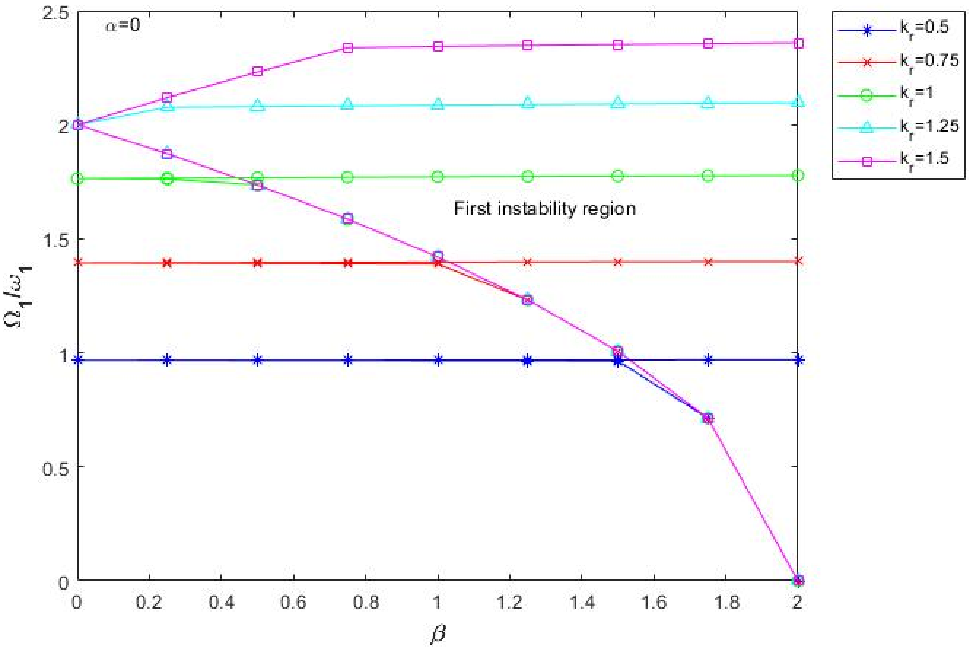

Figure 6.5 Effects of the number and stiffness coefficient of suspended spring-mass systems on the first stability regions of the one-bay frame structure with one spring-mass system and α=0

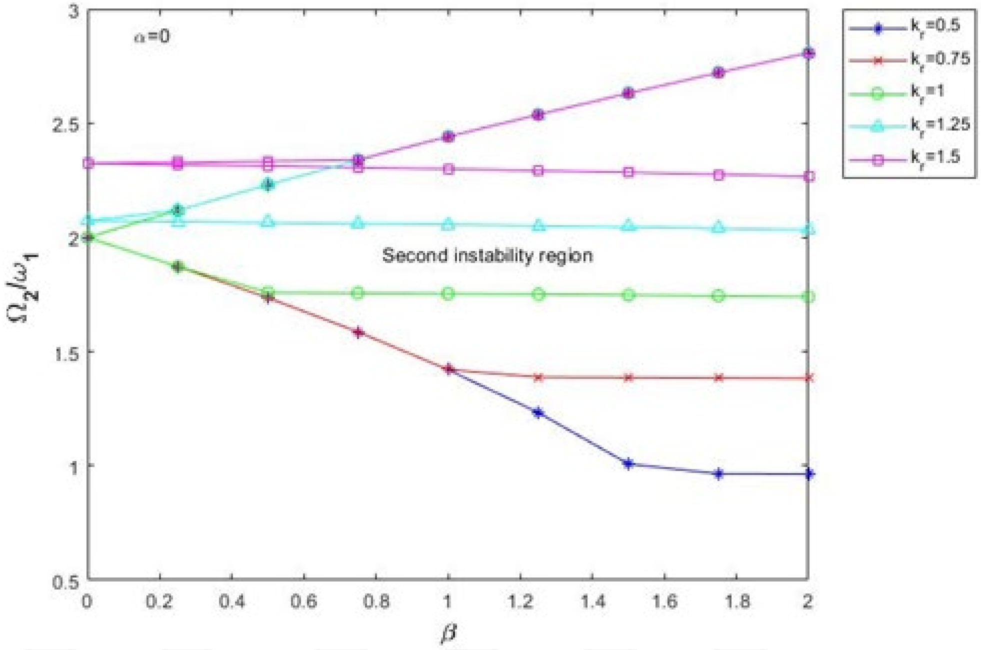

Figure 6.6 Effects of the number and stiffness coefficient of suspended spring-mass systems on the second stability regions of the one-bay frame structure with one spring-mass system and α=0

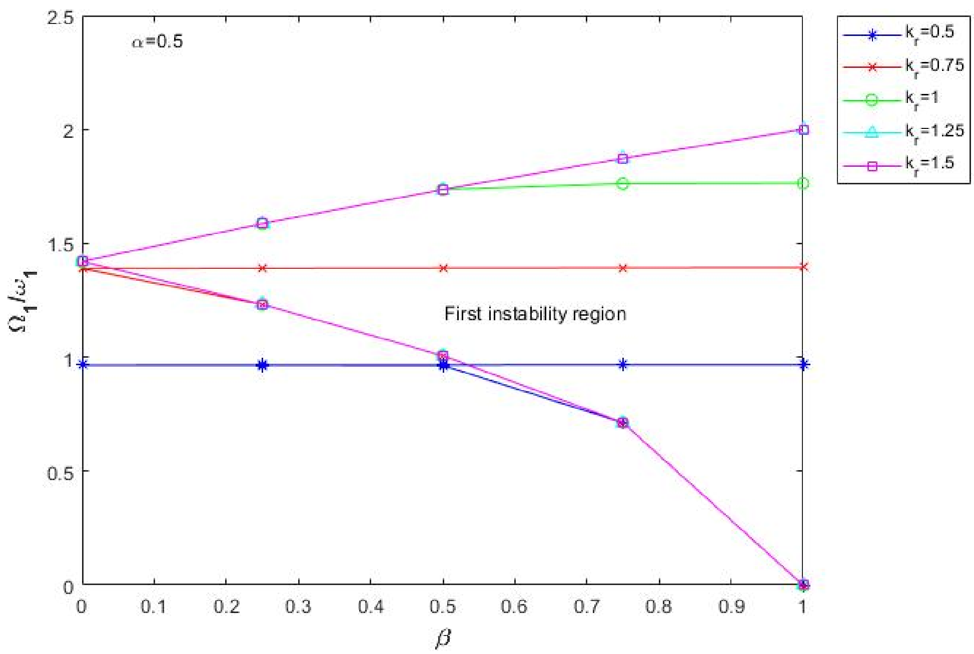

Figure 6.7 Effects of the number and stiffness coefficient of suspended spring-mass systems on the first stability regions of the one-bay frame structure with one spring-mass system and α=0.5

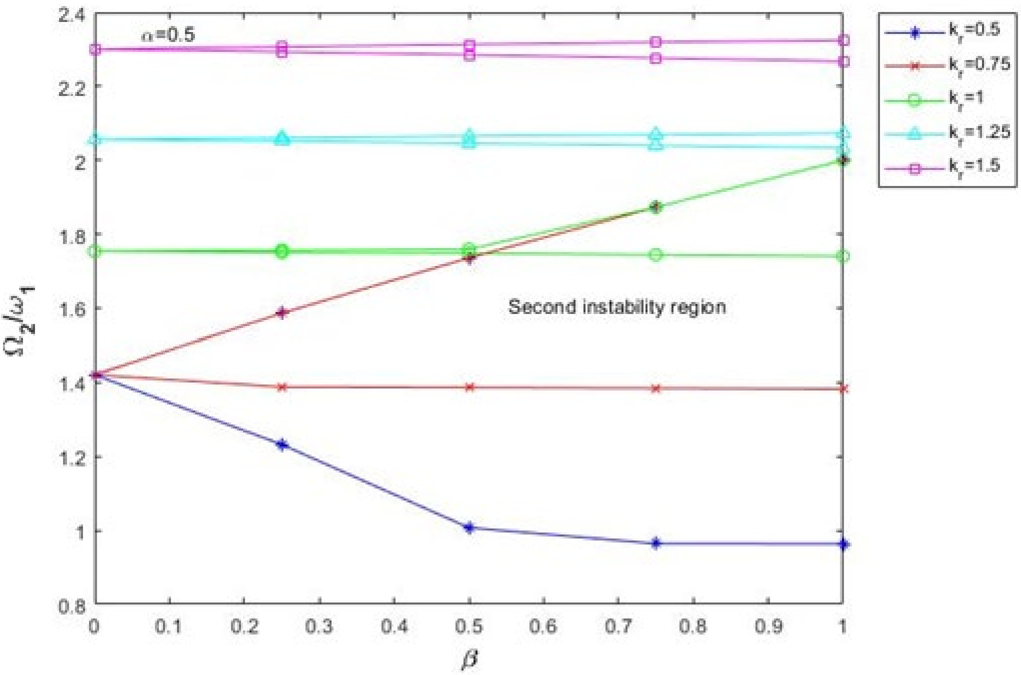

Figure 6.8 Effects of the number and stiffness coefficient of suspended spring-mass systems on the second stability regions of the one-bay frame structure with one spring-mass system and α=0.5

In Figures 6.9- 6.12, effects of two suspended spring-mass systems on the dynamic stability region of two-bay frame structures are given. Figures 6.9 and 6.10 show the first and second regions of instability in the absence of static loading. Figures 6.11 and 6.12 show the regions of instability for static loading.

When Figure 6.5 and Figure 6.9 are compared, it is seen that the first dynamic instability region is similar and there is almost no change. When Figure 6.6 and Figure 6.10 are compared, it is understood that there are differences in the dynamic instability regions, the dynamic stability region in Figure 6.10 has narrowed. The same results are observed for Figure 6.11 and Figure 6.12.

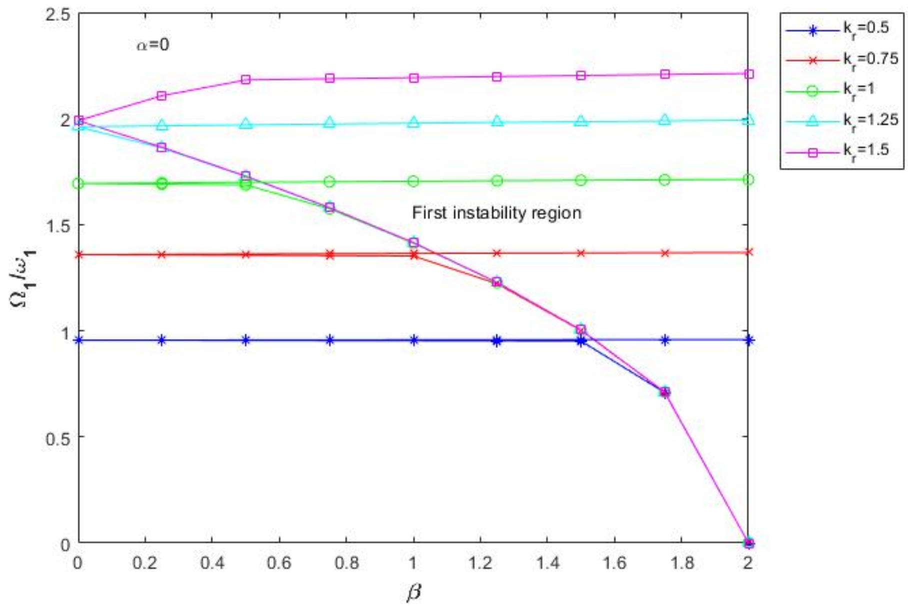

Figure 6.9 Effects of the number and stiffness coefficient of suspended spring-mass systems on the first stability regions of the one-bay frame structure with two spring-mass systems and α=0

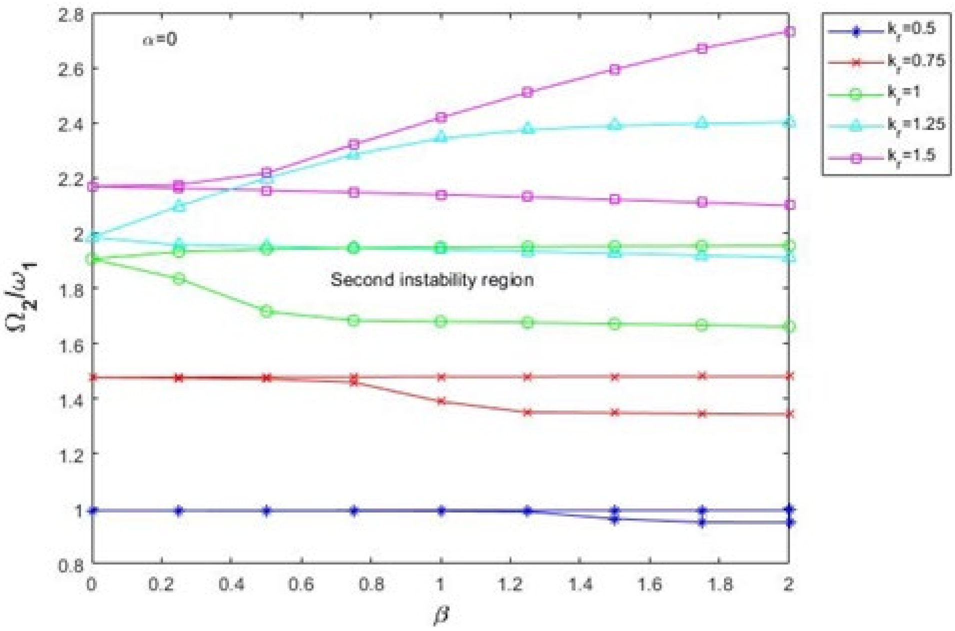

Figure 6.10 Effects of the number and stiffness coefficient of suspended spring-mass systems on the second stability regions of the one-bay frame structure with two spring-mass systems and α=0

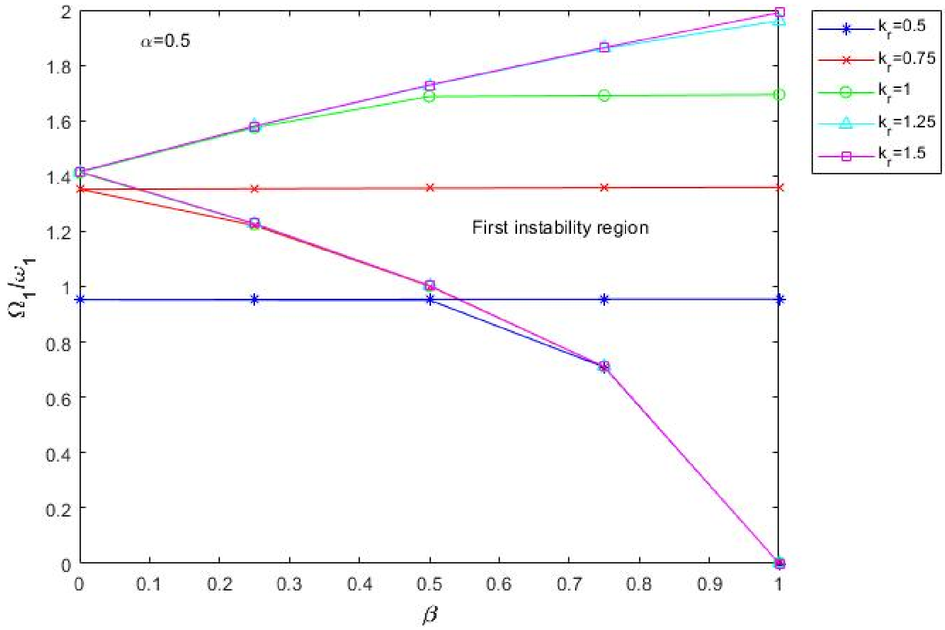

Figure 6.11 Effects of the number and stiffness coefficient of suspended spring-mass systems on the first stability regions of the one-bay frame structure with two spring-mass systems and α=0.5

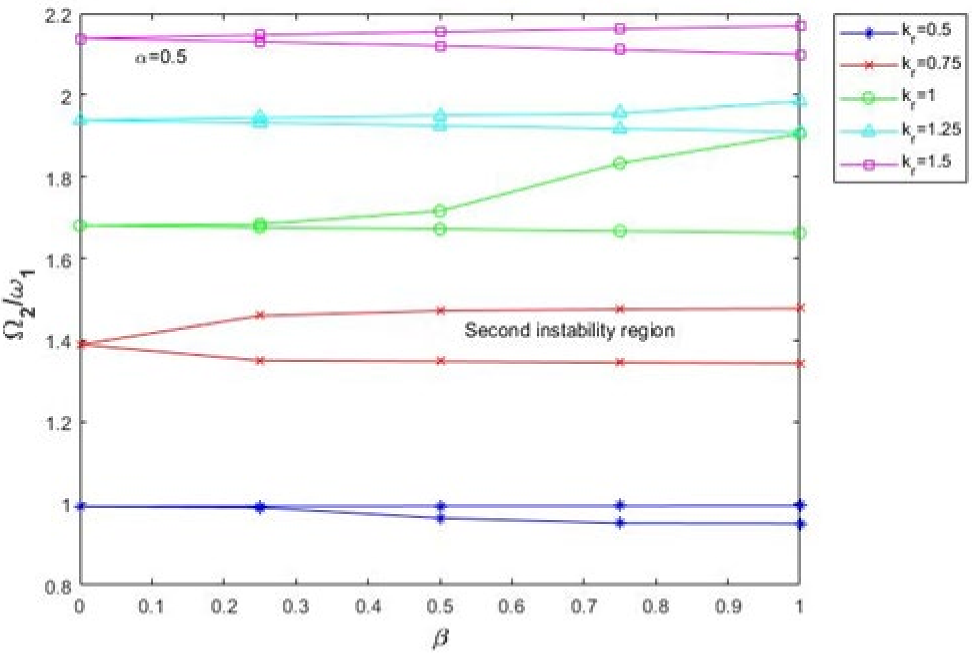

Figure 6.12 Effects of the number and stiffness coefficient of suspended spring-mass systems on the second stability regions of the one-bay frame structure with two spring-mass systems and α=0.5

In Figures 6.13- 6.16, effects of the frame structure of the three suspended spring-mass system on the dynamic stability region is given. Figures 6.13 and 6.14 show the first and second regions of instability in the absence of static loading. Figures 6.15 and 6.16 show the regions of instability for static loading.

It has been observed that the graphs obtained by suspended two spring-masses on the frame structure and the graphs obtained with three spring-mass suspending situations are similar, and there are no changes in the dynamic instability regions. It is analyzed that suspending more than two suspended spring-masses on the frame structure has no effect on the dynamic instability region.

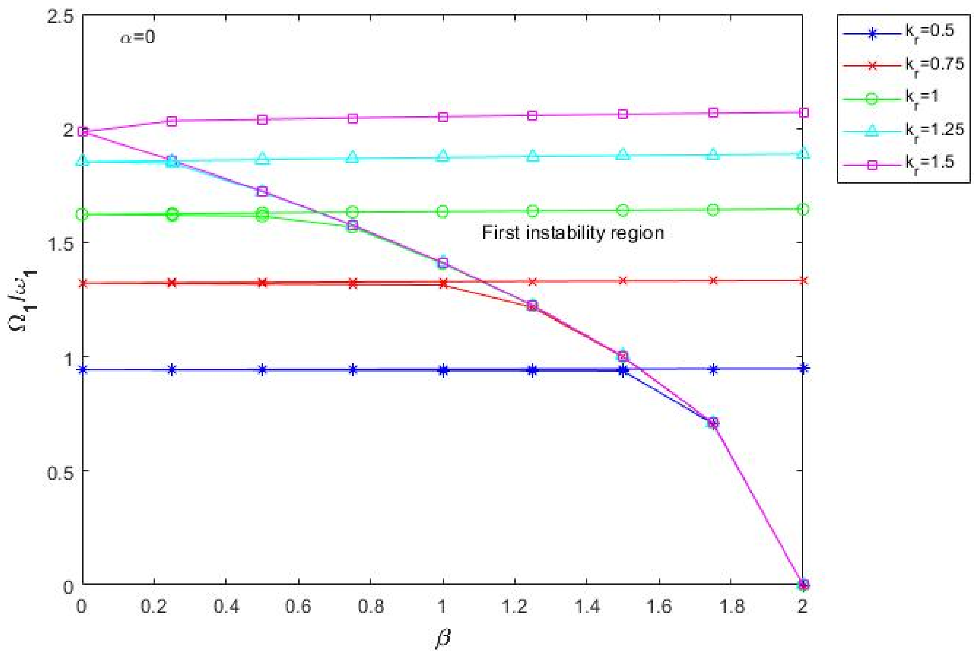

Figure 6.13 Effects of the number and stiffness coefficient of suspended spring-mass systems on the first stability regions of the one-bay frame structure with three spring-mass systems and α=0

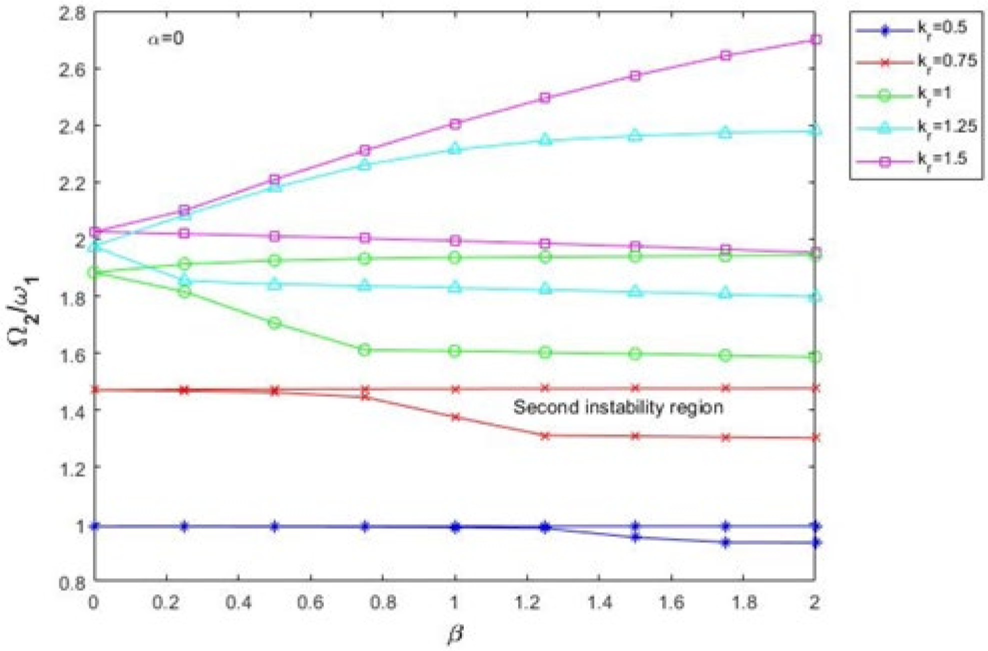

Figure 6.14 Effects of the number and stiffness coefficient of suspended spring-mass systems on the second stability regions of the one-bay frame structure with three spring-mass systems and α=0

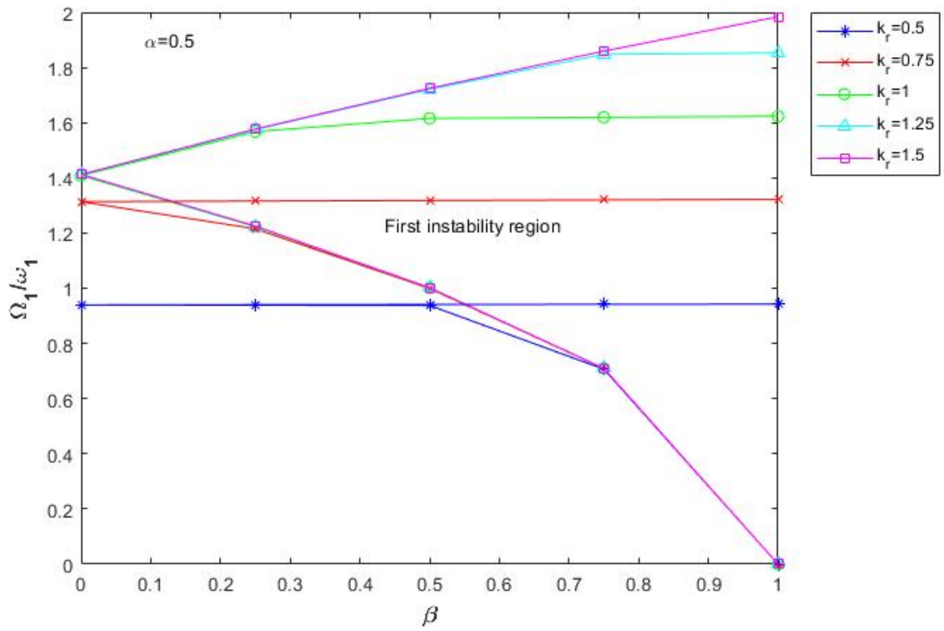

Figure 6.15 Effects of the number and stiffness coefficient of suspended spring-mass systems on the first stability regions of the one-bay frame structure with three spring-mass systems and α=0.5

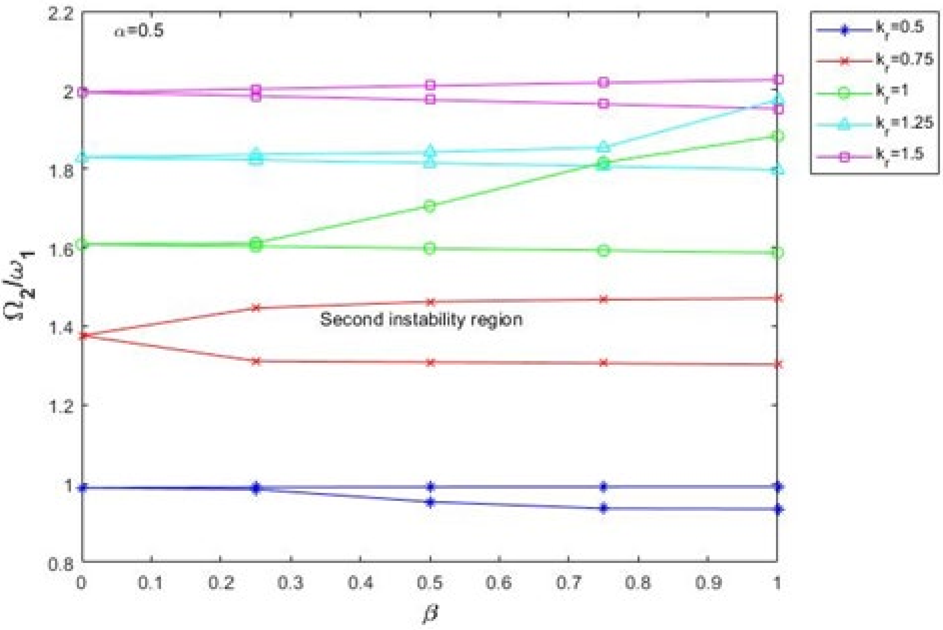

Figure 6.16 Effects of the number and stiffness coefficient of suspended spring-mass systems on the second stability regions of the one-bay frame structure with three spring-mass systems and α=0.5

6.3 Effects of the Number and Stiffness Coefficient of Suspended Spring-Mass System on the Two-Bay Frame Structures

In this section, effects of the number of suspended spring-mass systems and the stiffness coefficient on the dynamic stability regions of the two-bay frame structures are investigated. Spring-mass systems are suspended symmetrically on all frame structures.

Results are given for two suspended spring-masses in Figures 6.17-6.20, for four suspended spring-masses in Figures 6.21-6.24, and for six suspended spring-masses in Figure 6.24-6.27.

Figures 6.17-6.21 and 6.24 shows the first instability regions for the absence of static loading. When these graphs were examined, it was seen that the results were close to each other. The width of the instability regions are close to each other.

Figures 6.18-6.22 and 6.25 show the second instability regions where static loading is zero. It is understood that the results are close to each other in these graphs and the instability regions are close to each other.

In case of static loading in frame systems, Figures 6.19-6.23 and 6.26 show the first instability regions and Figures 6.20-6.24 and 6.27 the second stability regions. It has been observed that the graphics are similar in themselves.

Analyzes have been designed such that the suspended spring-mass system is on each bay of the two-bay frame structures. Therefore, at least two spring-mass systems have been suspended to the two-bay frame structure. Considering this situation, the results of the two-bay frame structures and the one-bay frame structures were compared. In Chapter 6, studied effects of the suspended spring-mass system on one and two-bay frame structures and noticed that the mode shapes obtained from the two frame structures were similar and the natural frequency values were close. However, different results were obtained in the dynamic stability analysis performed for these frame structures. It has been observed that the dynamic instability regions are different when a spring-mass system is suspended on each bay of both frame structures. It has been found that the second instability regions of the two-bay frame structures are narrower than the second instability regions of the one-bay frame structures.

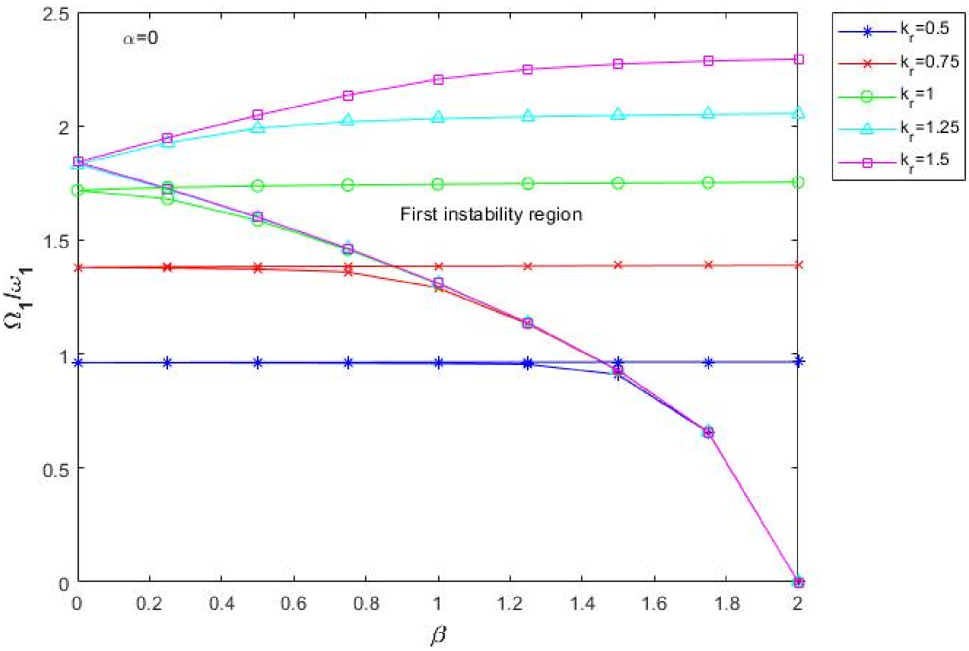

Figure 6.17 Effects of the number and stiffness coefficient of suspended spring-mass systems on the first stability regions of the two-bay frame structures with two spring-mass systems and α=0

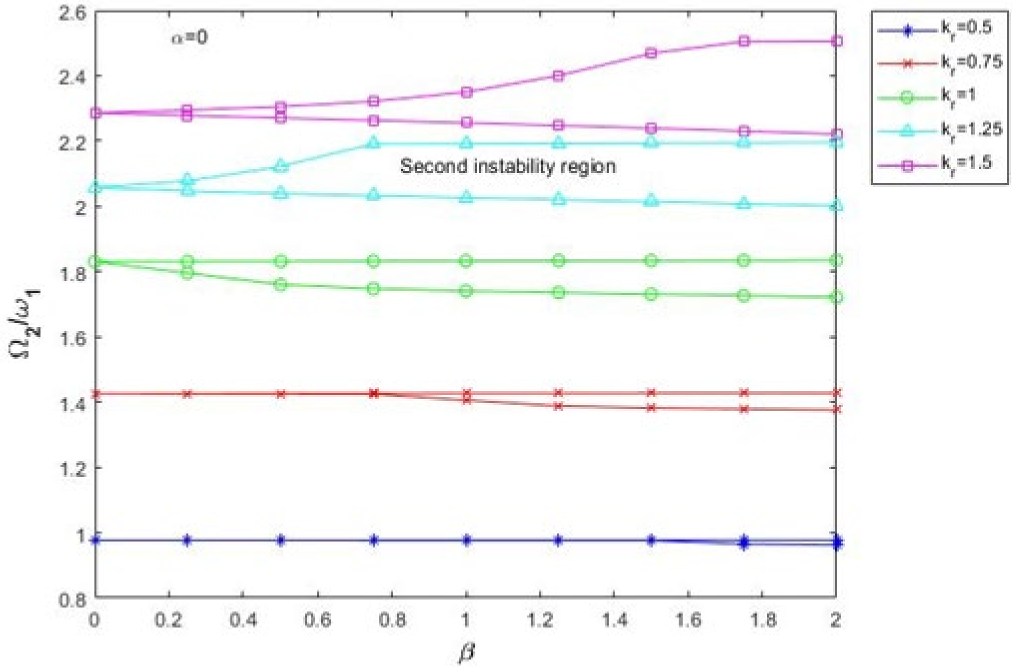

Figure 6.18 Effects of the number and stiffness coefficient of suspended spring-mass systems on the second stability regions of the two-bay frame structures with two spring-mass systems and α=0

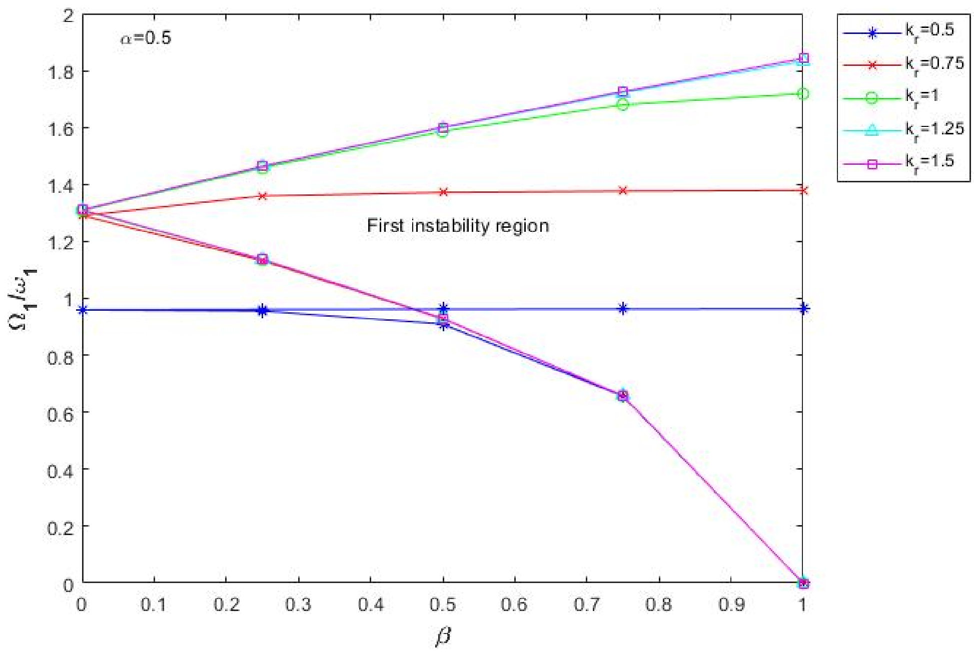

Figure 6.19 Effects of the number and stiffness coefficient of suspended spring-mass systems on the first stability regions of the two-bay frame structures with two spring-mass systems and α=0.5

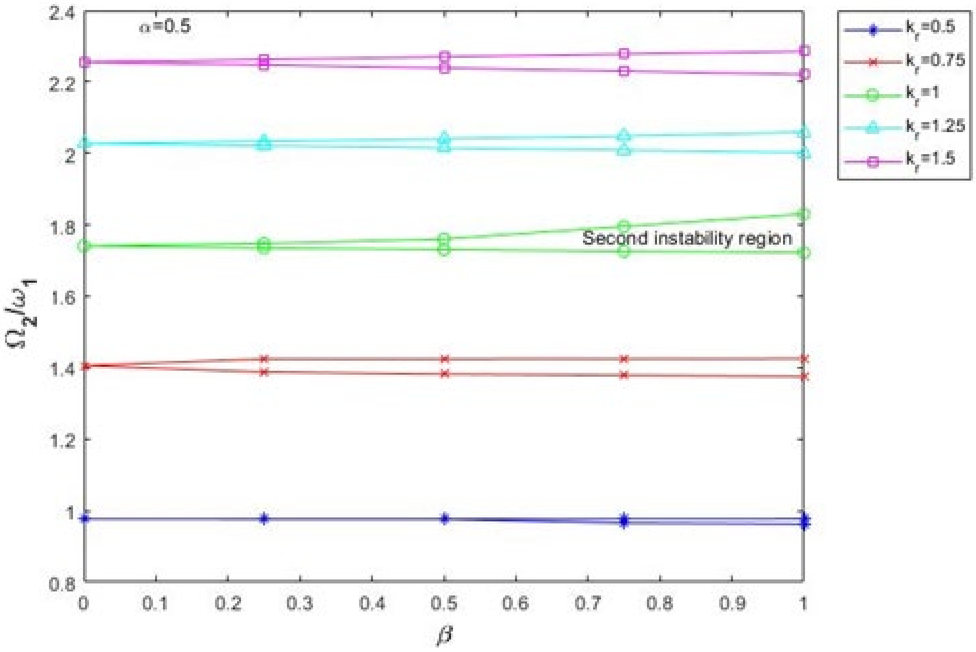

Figure 6.20 Effects of the number and stiffness coefficient of suspended spring-mass systems on the second stability regions of the two-bay frame structure with two spring-mass systems and α=0.5

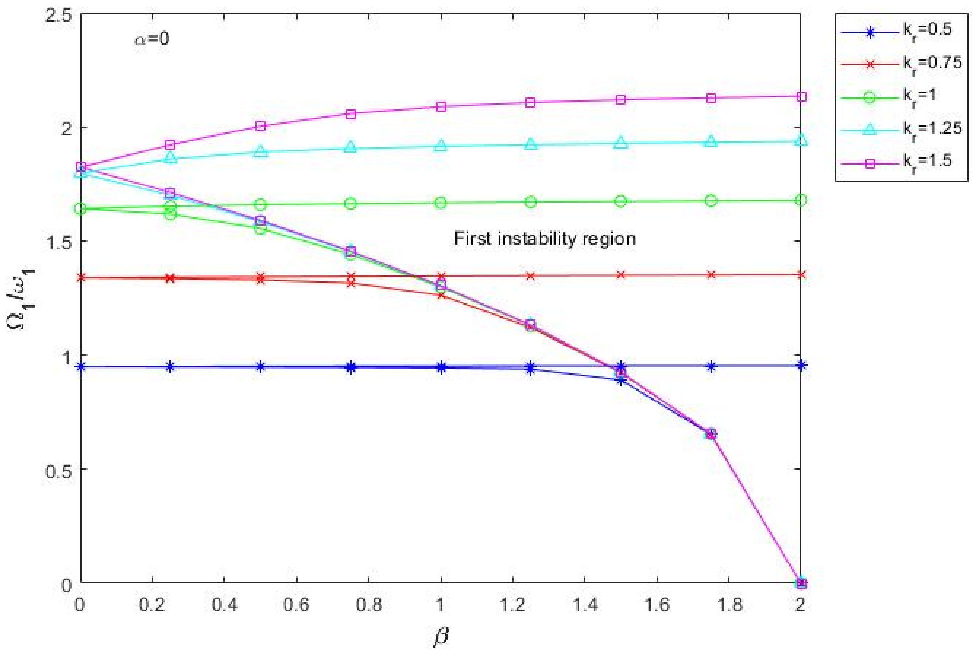

Figure 6.21 Effects of the number and stiffness coefficient of suspended spring-mass systems on the first stability regions of the two-bay frame structures with four spring-mass systems and α=0

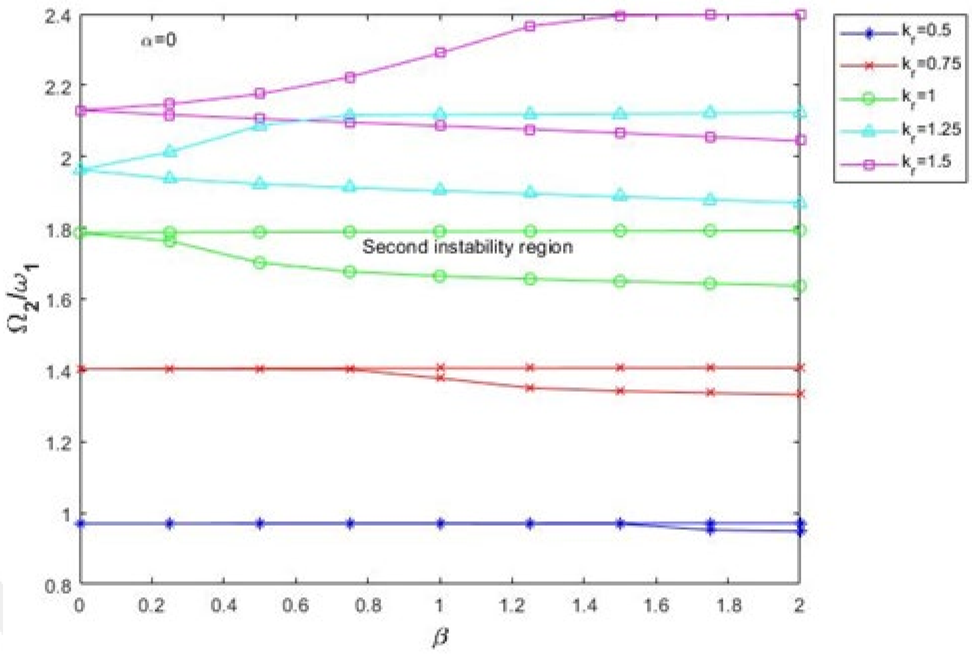

Figure 6.22 Effects of the number and stiffness coefficient of suspended spring-mass systems on the second stability regions of the two-bay frame structures with four spring-mass systems and α=0

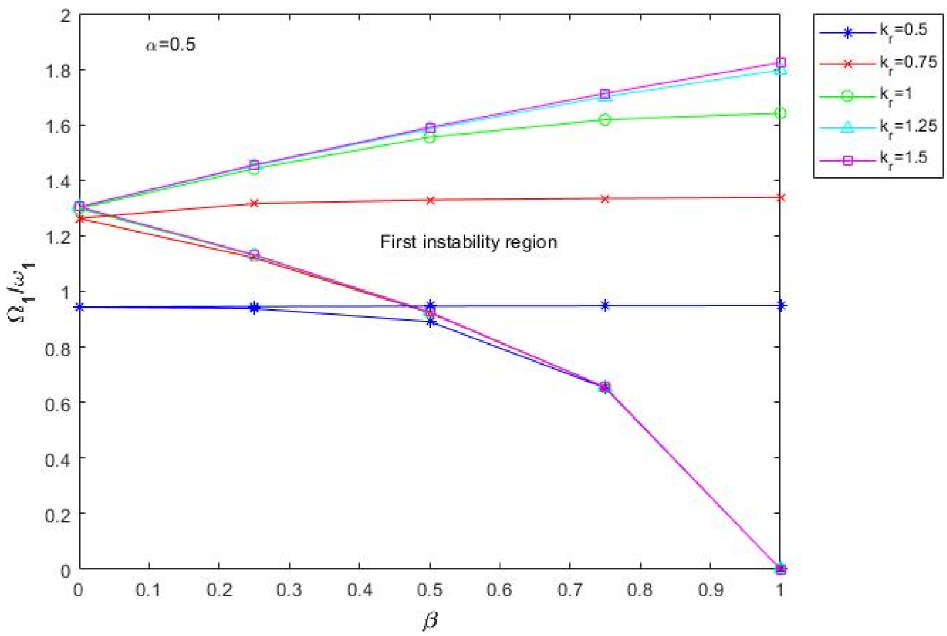

Figure 6.23 Effects of the number and stiffness coefficient of suspended spring-mass systems on the first stability regions of the two-bay frame structures with four spring-mass systems and α=0.5

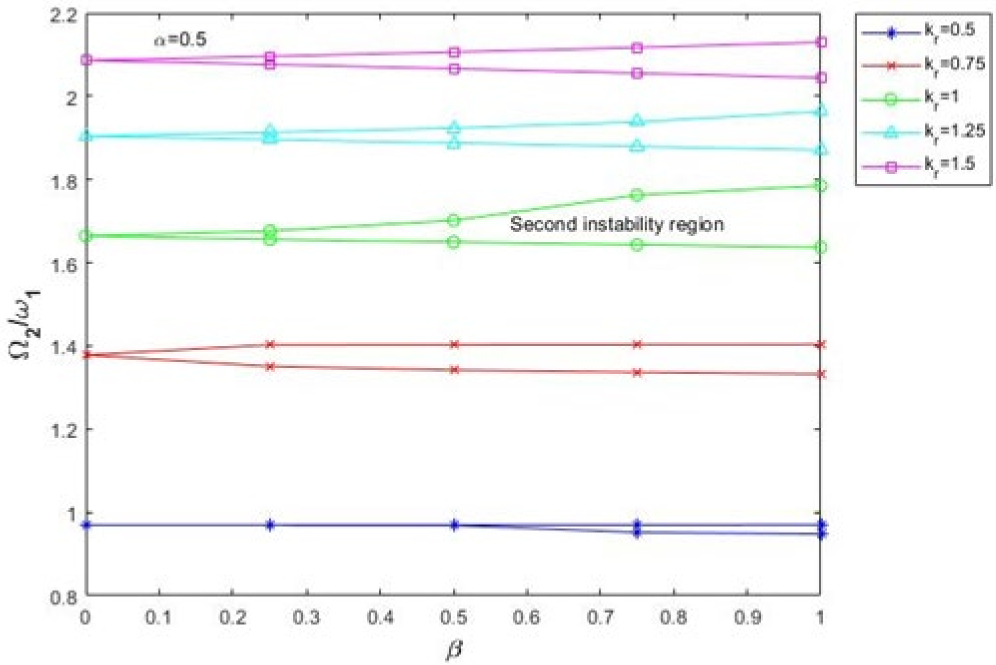

Figure 6.24 Effects of the number and stiffness coefficient of suspended spring-mass systems on the second stability regions of the two-bay frame structures with four spring-mass systems and α=0.5

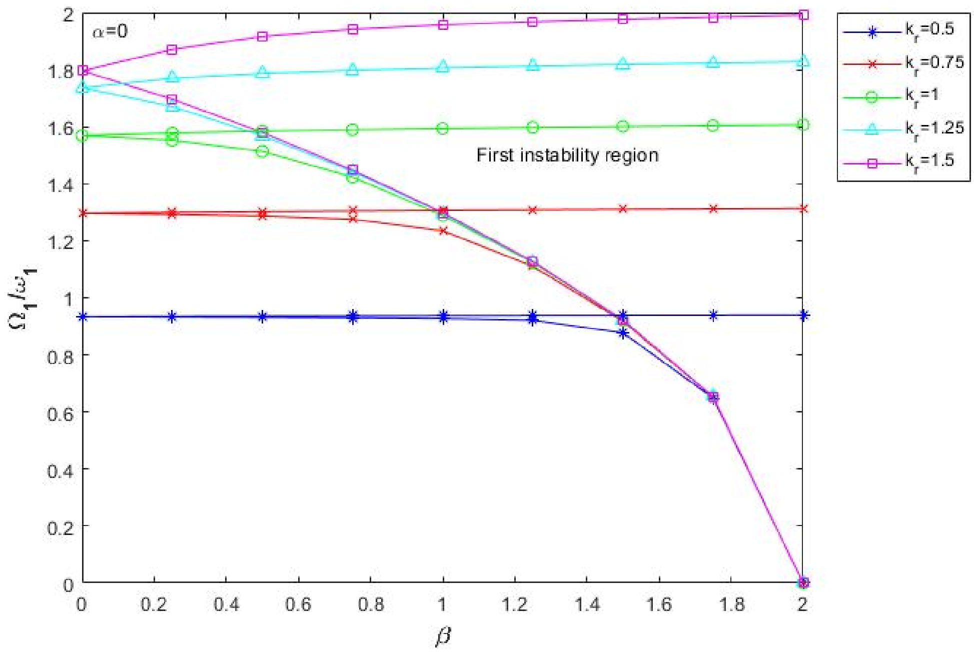

Figure 6.25 Effects of the number and stiffness coefficient of suspended spring-mass systems on the first stability regions of the two-bay frame structures with six spring-mass systems and α=0

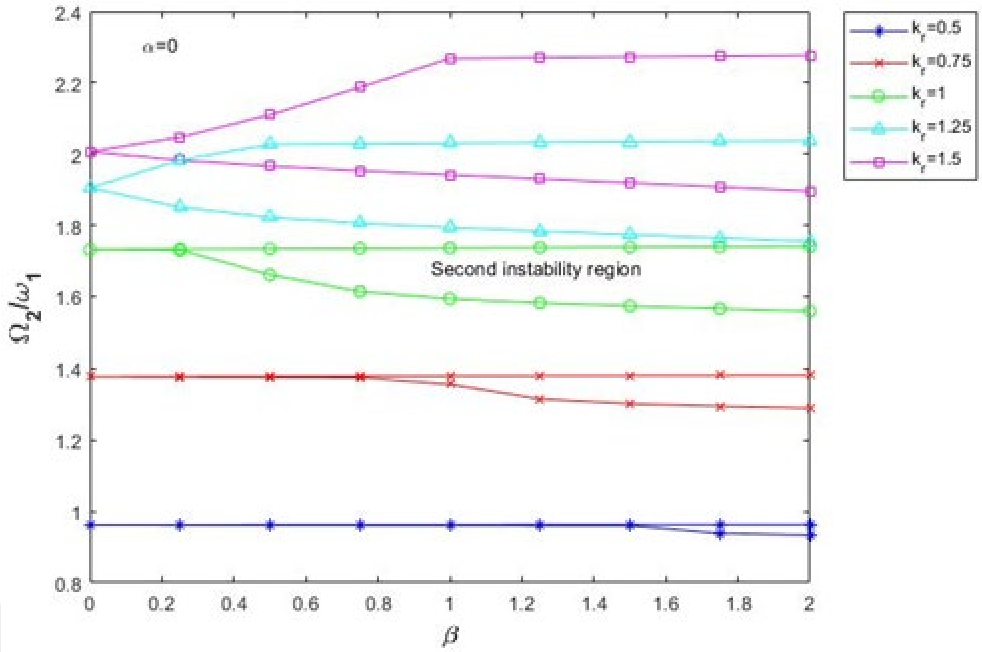

Figure 6.26 Effects of the number and stiffness coefficient of suspended spring-mass systems on the second stability regions of the two-bay frame structures with six spring-mass systems and α=0

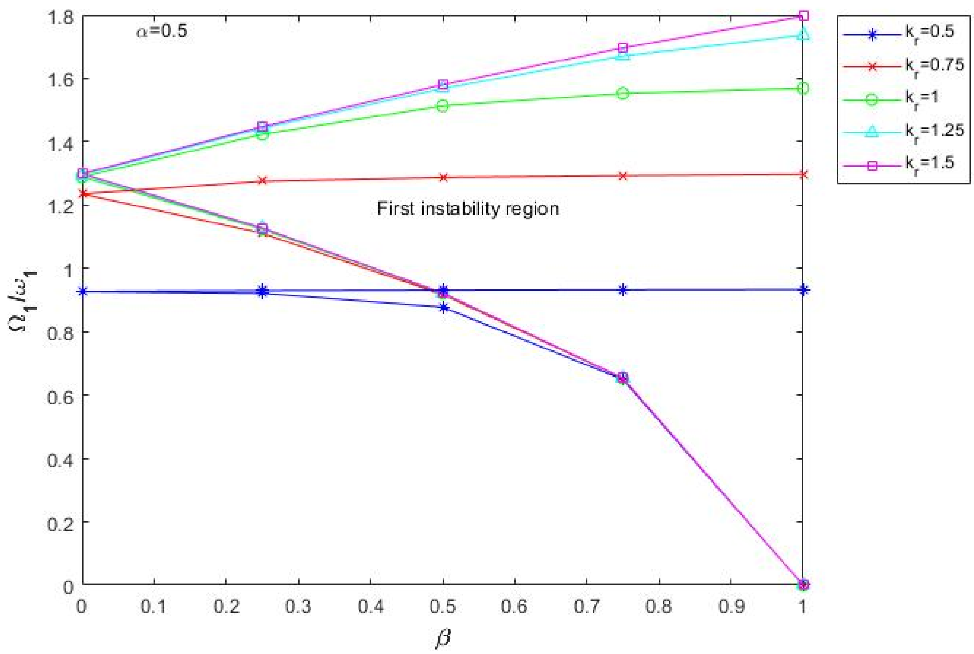

Figure 6.27 Effects of the number and stiffness coefficient of suspended spring-mass systems on the first stability regions of the two-bay frame structures with six spring-mass systems and α=0.5

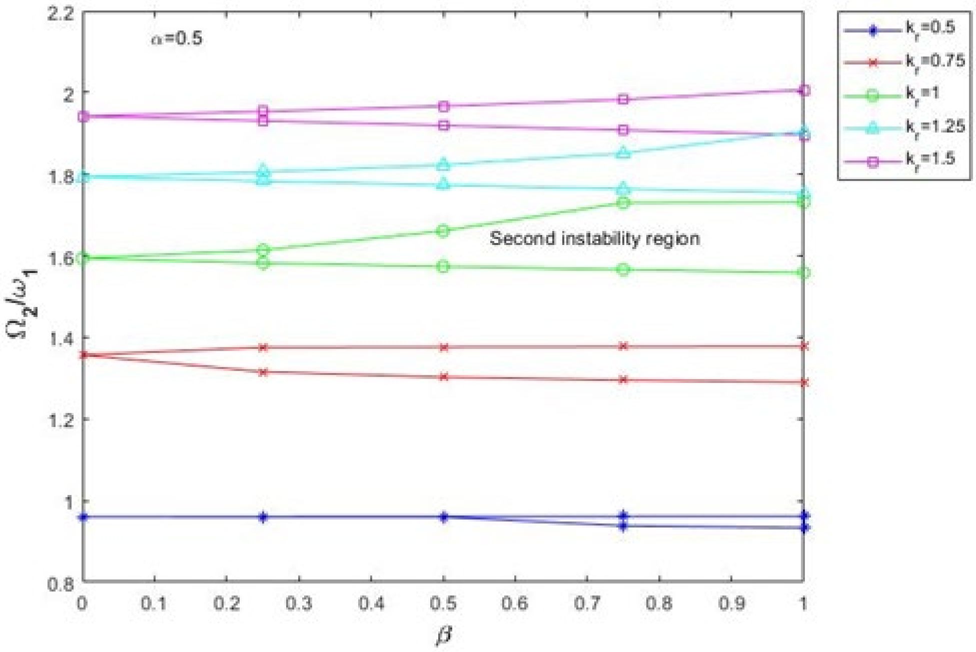

Figure 6.28 Effects of the number and stiffness coefficient of suspended spring-mass systems on the second stability regions of the two-bay frame structures with six spring-mass systems and α=0.5

6.4 Effects of the Asymmetric Suspended of the Spring-Mass Systems

In this section, dynamic stability under asymmetric suspending of spring-mass systems on frame structures is investigated. Asymmetric suspended single spring-mass and asymmetric suspended two spring-mass is given in Figure 6.29.

Figures 6.30-6.33 shows the instability regions when the single spring-mass is suspended. Figures 6.34-6.34 shows the results for the suspended case of two spring-mass systems.

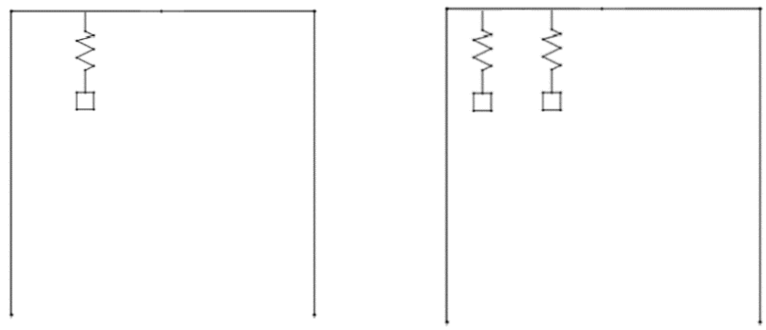

Figure 6.29 Asymmetric suspended single and double spring-mass systems on one-bay frames

When the results in this section are compared with the cases where the spring-mass system is suspended symmetrically (Figures 6.5-6.8 and Figures 6.9-6.12), it is seen that similar results are obtained. The most important difference was noticed in the graphs showing the second instability region. It was noticed that Ω/ω ratios increased as the kr value increased in asymmetric suspending. In this case, under the same conditions, it was seen that effects of symmetrical or asymmetric suspending of the spring-mass systems to the frame structures we examined on the dynamic stability of the frame structures could not be different.

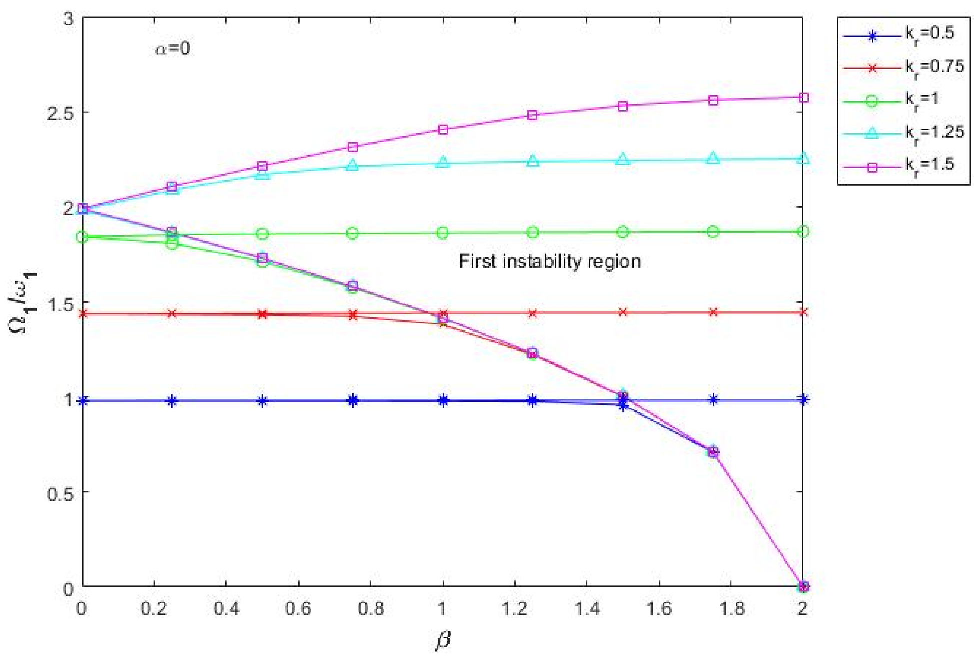

Figure 6.30 Effects of the asymmetric suspending of the spring-mass systems on the first stability regions of the one-bay frame structure with one spring-mass system and α=0

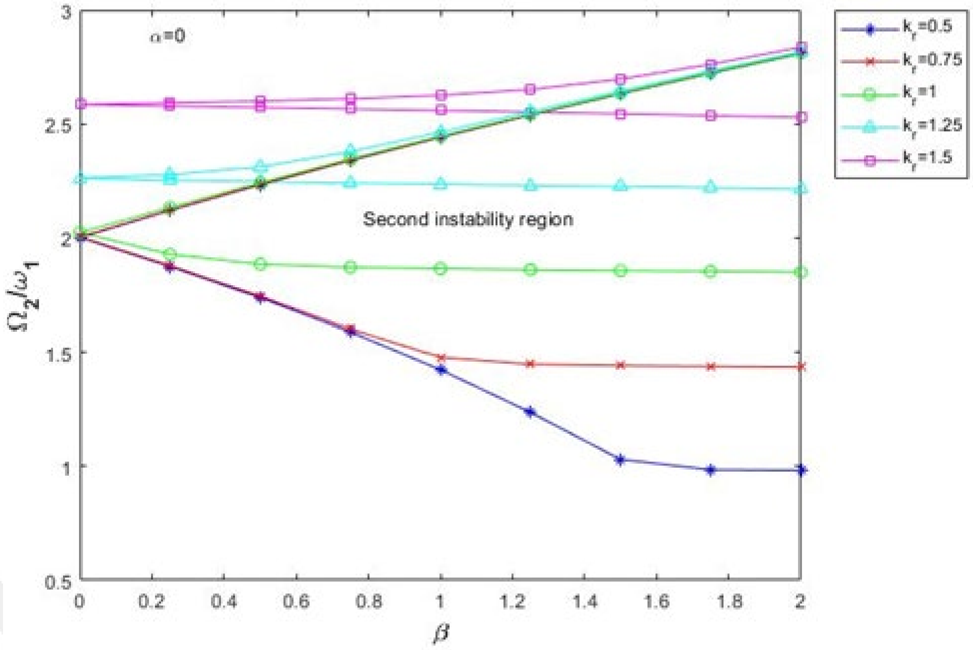

Figure 6.31 Effects of the asymmetric suspending of the spring-mass systems on the second stability regions of the one-bay frame structure with one spring-mass system and α=0

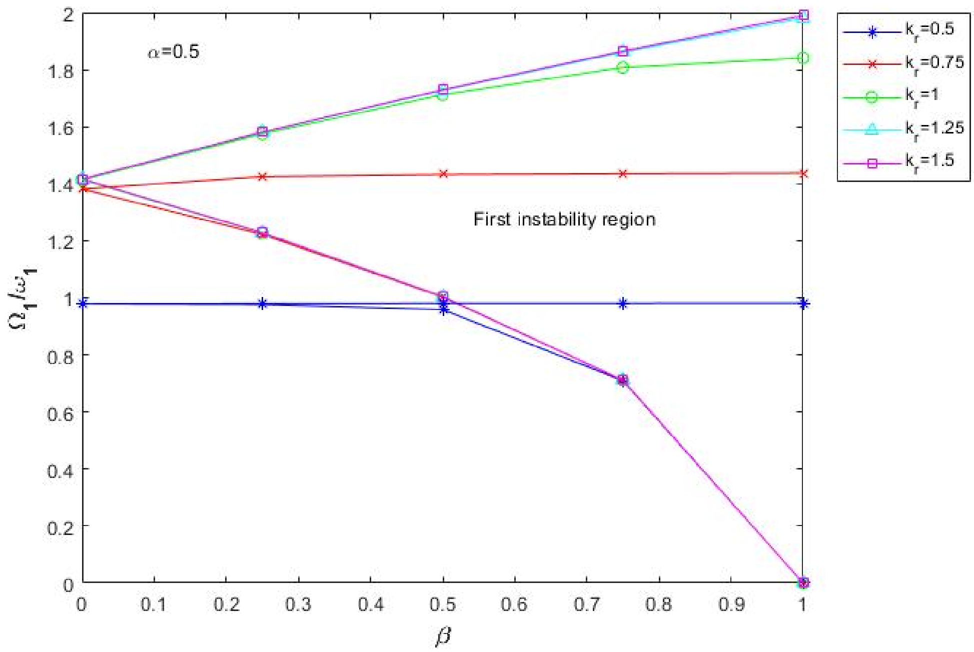

Figure 6.32 Effects of the asymmetric suspending of the spring-mass systems on the first stability regions of the one-bay frame structure with one spring-mass system and α=0.5

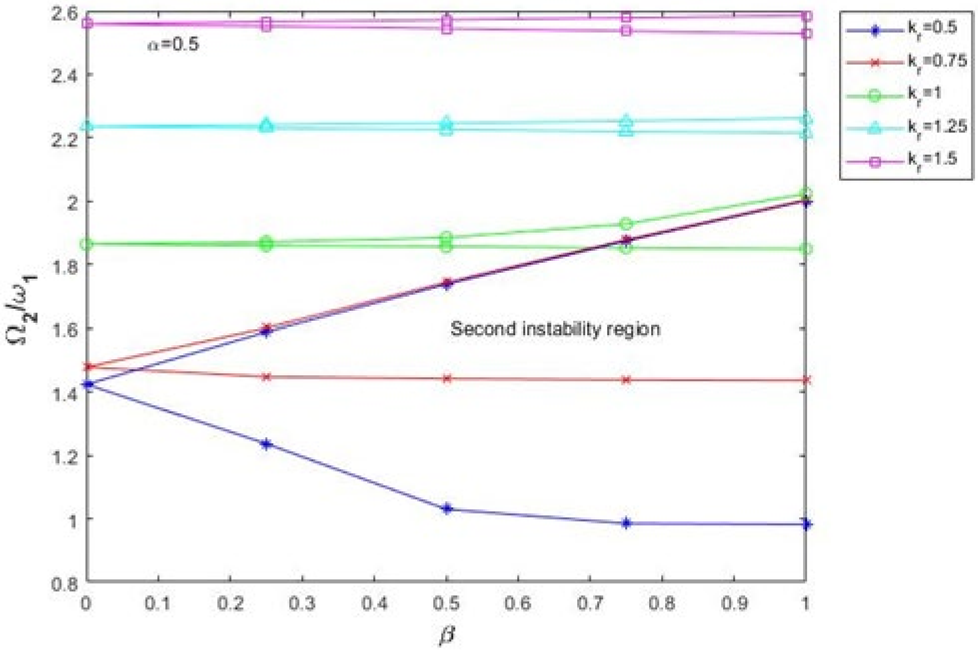

Figure 6.33 Effects of the asymmetric suspending of the spring-mass systems on the second stability regions of the one-bay frame structure with one spring-mass system and α=0.5

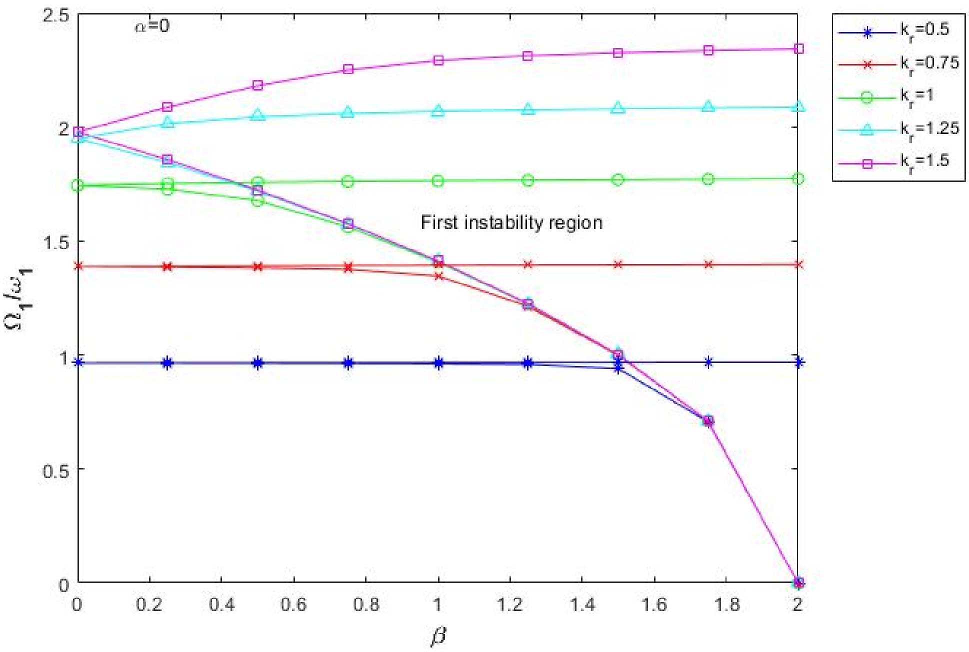

Figure 6.34 Effects of the asymmetric suspending of the spring-mass systems on the first stability regions of the one-bay frame structure with two spring-mass systems and α=0

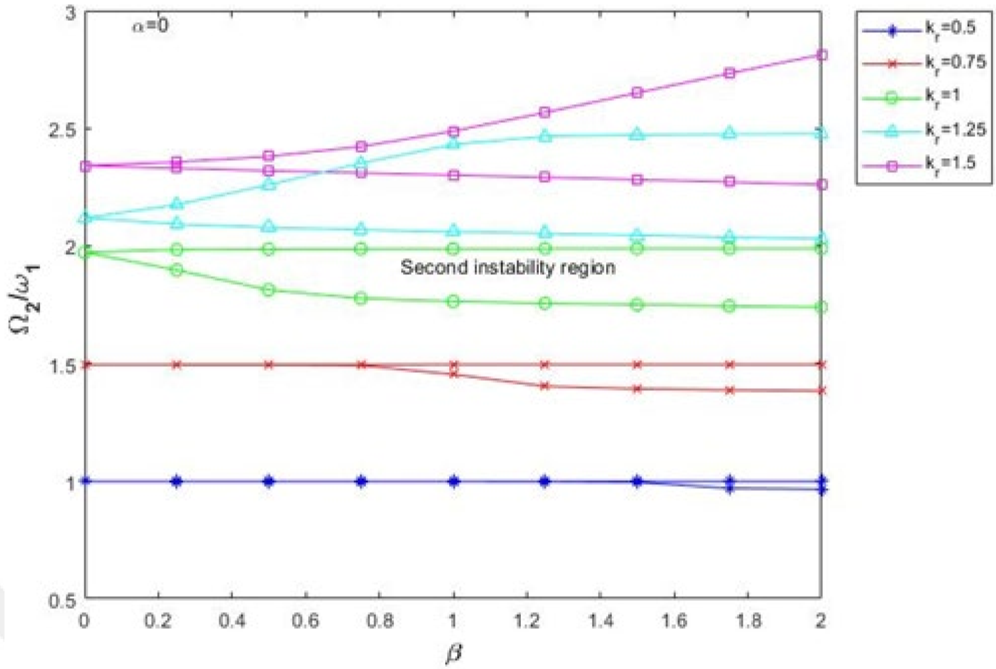

Figure 6.35 Effects of the asymmetric suspending of the spring-mass systems on the second stability regions of the one-bay frame structure with two spring-mass systems and α=0

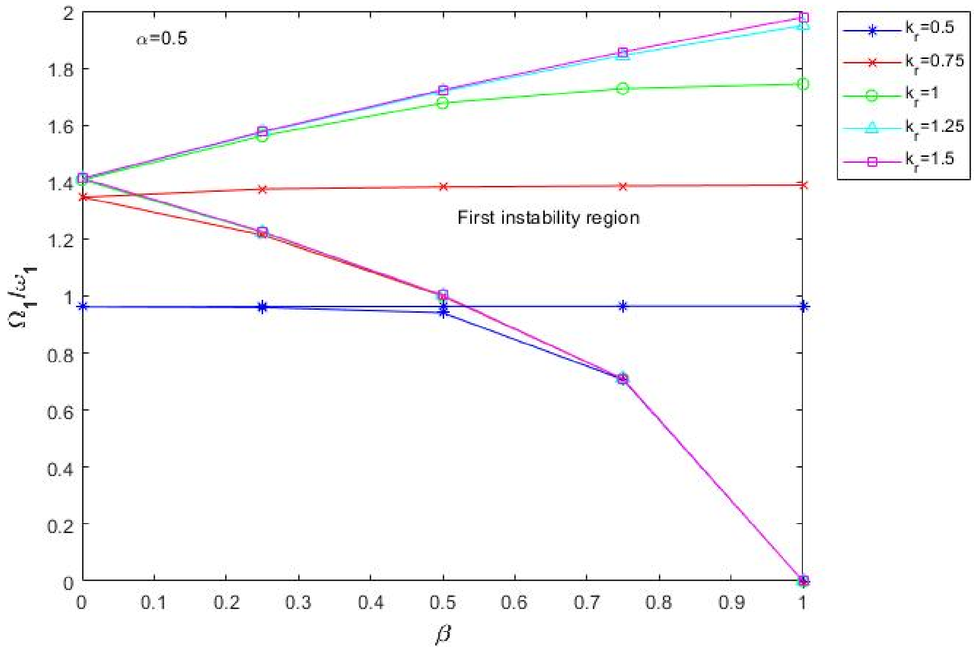

Figure 6.36 Effects of the asymmetric suspending of the spring-mass systems on the first stability regions of the one-bay frame structure with two spring-mass systems and α=0.5

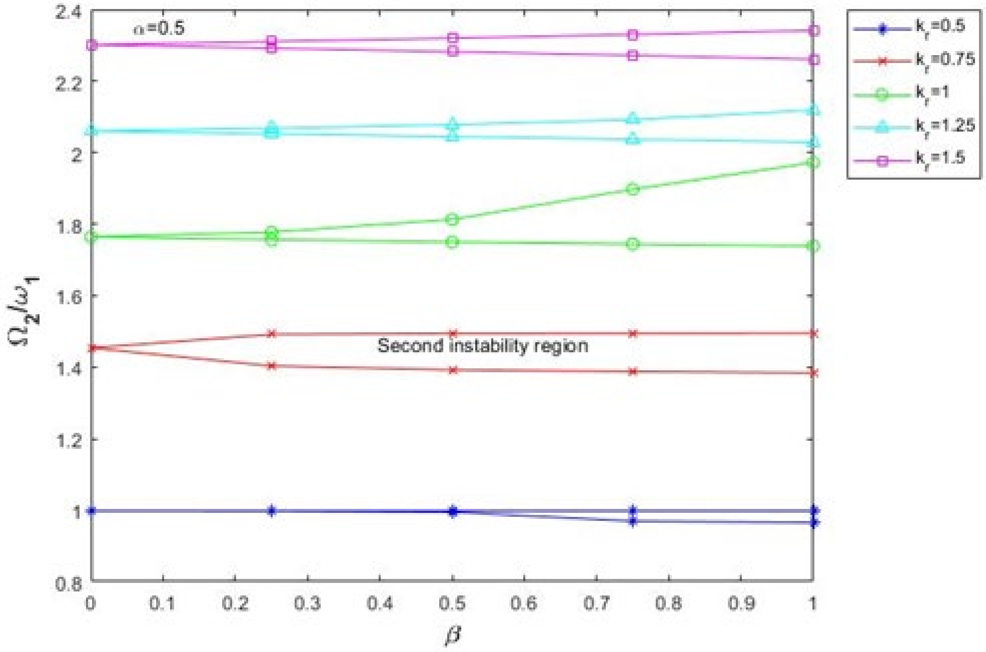

Figure 6.37 Effects of the asymmetric suspending of the spring-mass systems on the second stability regions of the one-bay frame structure with two spring-mass systems and α=0.5

CHAPTER SEVEN

CONCLUSION

In this study, effects of the suspended spring-mass systems on the in-plane natural frequencies, mode shapes and dynamic stability of frame structures were investigated. In the analysis, the number of bays, the number and location of the suspended spring-mass system and the spring stiffness parameters were considered as variables. The results obtained were compiled below:

- In all free vibration analyses, it was observed that the number of the mode shapes of the frame structures increased by the number of suspended spring-mass systems added to the frames.
- In the case of k_{s1} and k_{s2} are used, very small changes in the natural frequency values and mode shapes of the frame structure were observed. However, this effect does not disrupt the mode characteristic.
- In the case of k_{s1} and k_{s2} are used, it is understood that adding more than one suspended spring-mass system to the frame structures does not change the natural frequencies and mode shapes of frame structures. Likewise, increasing the number of bay of the frame structure did not change the natural frequency analysis results.
- In the case of k_{s3} is used, it has been observed that no mode shape occurs in which only the suspended spring-mass system is dominant. The suspended spring-mass system is displaced depending on the beam element.
- It is seen in all analysis results that the suspended spring-mass system does not have an effect on the natural frequencies of the frame systems when the where beam element does not displacement in the vertical direction. Similarly, it is observed that the suspended spring-mass system has no effect when suspended spring-mass systems are suspend on nodes where the beam element has no vertical movement.
- It is understood that the increase in the number of bays changes the dynamic instability region, but the effect is mostly in the second dynamic instability

region. In addition, it is observed that the second dynamic instability region is narrower than the first dynamic instability region. When the static load parameter was 0.5, it was seen that the value of the frequency rates decreased and the region of instability became narrower.

- When the single spring-mass system is suspended on the frame structures, it is seen that the first dynamic instability region shrinks depending on the k_r value. It was observed that the narrowing in the dynamic instability region increased as the k_r decreased. It was observed that it also contracted in the second dynamic instability region, but it was noticed that the higher the k_r value, the greater the contraction in the dynamic instability region. The same is observed in the case where the static load parameter is 0.5.
- When comparing two or more spring-mass systems that were suspended on the frame structures and the single spring-mass system suspended situation, it was observed that there was no change in the first dynamic instability region. However, the change in the second dynamic instability region is greater and the region of dynamic instability narrowed.
- When examining the results for the two-bay frame structures, it was found that they were similar to the results of one-bay frame structures with multiple suspended spring-mass systems. None of the results obtained for the two-bay frames are similar to the results of a one-bay frame structure loaded with a single suspended spring-mass system.
- When the asymmetric suspending of the spring-mass systems is examined, it is seen that the Ω/ω ratios increase as the value of k_r increases in the graphs showing the second dynamic instability region.
- When all dynamic stability analyzes are considered, it has been observed that suspending more than two spring-mass systems on the frame structures does not affect the dynamic instability regions of the frame structures.

In subsequent studies, it may be considered to examine the effect of a crack or moving load on the dynamic stability of the structures examined in this study.

REFERENCES

Abbas, B.A.H. (1977). *Mechanical vibration and dynamic stability of complex structures by finite element method*. Ph.D. Thesis, Surrey University, Surrey.

Airbus (2020). Retrieved January 15, 2020, from https://www.airbus.com/.

Bolotin, V.V. (1962). *The dynamic stability of elastic systems*. San Francisco: HoldenDay, Inc.

Briseghella, L., Majorana, C. E., & Pellegrino, C. (1998). Dynamic stability of elastic structures: a finite element approach. *Computers & Structures, 69* (1), 11-25.

Erkan, H., Öztürk, H., & Sabuncu, M. (2013). Çok bölmeli çerçevelerin düzlem içi ve dışı serbest titreşimleri. *Symposium: 16. Ulusal Makine Teorisi Sempozyumu*, 222-232.

Erkan, H., Öztürk, H., & Demirtaş, S. (2019). Asılı kütle-yay sisteminin çerçeve yapıların düzlem içi doğal frekansları ve titreşim biçimleri üzerindeki etkileri. *Symposium: 19. Ulusal Makine Teorisi Sempozyumu*, 353-361.

Griesmer, A. (2014). *Size Parameters for Free Tetrahedral Meshing in COMSOL Multiphysics*. Retrieved January 30, 2014, from https://www.comsol.com/blogs/size-parameters-free-tetrahedral-meshing-comsol-multiphysics/.

Gürgöze, M. (1996). On the eigenfrequencies of a cantilever beam with attached tip mass and a spring-mass system. *Journal of Sound and Vibration, 190* (2), 149-162.

Hutton D. V. (2004). *Fundamentals of Finite Element Analysis*. New York: McGraw-Hill

İbrahem, A. M. (2010). *Vibration analysis of cracked frame structure*. Msc Thesis, Dokuz Eylül Üniversitesi, İzmir.

Ji, J., Hong, R., Sun, F., & Huang, X. (2018). Thermal characteristic analysis of Z-axis guideway based on thermal contact resistance. *Advances in Mechanical Engineering, 10* (10), 987-1015

Kapur, K.K. (1966). Vibrations of a Timoshenko beam, using finite element approach. *Journal of Acoustical Society of America, 40* (5), 1058-1063.

Kawashima, S., & Fijimato, T. (1984). Vibration analysis of frame with semi-rigid connections. *Computers & Structures, 19* (1,2), 85-92.

Liu, G.R., & Quek, S. S. (2003). *The Finite Element Method*. Oxford: Butterworth Heinemann

Lee, H.P., & HG, T.Y. (1994). In-plane vibration of planar frame structures. *Journal of Sound and Vibration*, *172* (3), 420-427.

Mei, C. (2012). Free vibration analysis of classical single-story multi-bay planar frames. *Journal of Vibration and Control, 19* (13), 2022-2035.

Öztürk, H., Yashar, A. & Sabuncu, M. (2016). Dynamic stability of cracked multi-bay frame structures. *Mechanics of Advanced Materials and Structures, 23 (6), 715-726.*

Qiao, H., Li, Q.S., & Li, G.Q. (2002). Vibratory characteristics of exural non-uniform Euler-Bernoulli beams carrying an arbitrary number of spring-mass systems. *International Journal of Mechanical Sciences, 44* (4), 725-743.

Sarsmaz, P. (2016). *Vibration analyses of complex structureal members with various torsional spring foundations and suspended spring-mass systems*. Master Thesis, Dokuz Eylül University, İzmir.

Thomas, J. & Abbas, B.A.H. (1975). Finite element model for dynamic analysis of Timoshenko beam. *Journal of Sound and Vibration, 41* (3), 291-299.

Thomas, J., & Abbas B.A.H (1976). Dynamic stability of timoshenko beam by finite element method. *Journal of Engineering for Industry, Transactions of the ASME, 89* (1), 1145-1151.

Thomas, J., & Belek, H.T. (1977). Free vibration of blade packets. *Journal Mechanical Engineering Science, 19* (1), 13-21.

Vatan, S. (2019). *Dynamic stability analysis of a curved beam with suspended spring-mass systems*. Master Thesis, Dokuz Eylül University, İzmir.

APPENDICES

NOMENCLATURE

A	cross-sectional area of the curved beam
E	elasticity module of the column and beam
I_{xx}	moment of area of cross-section of the column and beam
k_s	suspended stiffness coefficient
k_{cr}	ratio critical buckling load parameter
K_e	global elastic stiffness matrix
K_g	global geometric stiffness matrix
k_e	elastic stiffness matrix of the elemental finite element
k_{ratio}	ratio of the stiffness coefficients
L	transformation matrix
ℓ	length of the finite element
m_s	suspended mass
M	global mass (inertia) matrix
m_e	mass matrix of the elemental finite element
$P(t)$	periodic load
P_{cr}	critical buckling load
q	generalized coordinates
T	kinetic energy
U	strain energy
α	static load parameter

β	dynamic load parameter
ρ	density of the curved beam
φ	the opening angle of the finite element
ψ	rotation of tangent
Ω	disturbing frequency
ω	the natural frequency